

# Chiral-logarithmic Corrections to the $S$ and $T$ Parameters in Higgsless Models

S. Dawson and C. B. Jackson<sup>y</sup>

Physics Department, Brookhaven National Laboratory, Upton, NY 11973-5000, USA

(Dated: February 8, 2020)

## Abstract

Recently, Higgsless models have proven to be viable alternatives to the Standard Model (SM) and supersymmetric models in describing the breaking of the electroweak symmetry. Whether extra-dimensional in nature or their deconstructed counterparts, the physical spectrum of these models typically consists of "towers" of massive vector gauge bosons which carry the same quantum numbers as the SM  $W$  and  $Z$ . In this paper, we calculate the one-loop, chiral-logarithmic corrections to the  $S$  and  $T$  parameters from the lightest (i.e. SM) and the next-to-lightest gauge bosons using a novel application of the Pinch Technique. We perform our calculation using generic Feynman rules with generic couplings such that our results can be applied to various models. To demonstrate how to use our results, we calculate the leading chiral-logarithmic corrections to the  $S$  and  $T$  parameters in the deconstructed three site Higgsless model. As we point out, however, our results are not exclusive to Higgsless models and may, in fact, be used to calculate the one-loop corrections from additional gauge bosons in models with fundamental (or composite) Higgs bosons.

---

<sup>E</sup>lectronic address: dawson@quark.phy.bnl.gov

<sup>y</sup><sup>E</sup>lectronic address: cbjackson@bnl.gov

## I. INTRODUCTION

The source of electroweak symmetry breaking (EWSB), i.e. the generation of the  $W$  and  $Z^0$  masses, remains as one of the unanswered questions in particle physics. If the Standard Model (SM) or one of its supersymmetric (SUSY) extensions are correct, then one (or more)  $SU(2)$  scalar doublets are responsible for EWSB and at least one physical Higgs boson should be discovered at the Large Hadron Collider (LHC).

Unfortunately, the Higgs mechanism as implemented in the SM has several theoretical shortcomings. The most troublesome of these is the fact that the Higgs boson mass is unstable against radiative corrections, a situation known as the large hierarchy problem. In other words, for the Higgs boson to be light (as indicated by electroweak precision measurements), its bare mass must be highly  $\text{fine-tuned}$  to cancel large loop effects from high-scale physics. In SUSY extensions, this  $\text{fine-tuning}$  is avoided due to additional particles which cancel the quadratic contributions to the Higgs boson mass from SM particles.

In the past several years, an interesting alternative to SUSY models has emerged in the form of extra-dimensional models [1, 2]. In most of these scenarios, the size and shape of the extra dimension(s) are responsible for solving the large hierarchy problem. In addition, variations of these models can also provide viable alternatives to the Higgs mechanism. For example, in models where the SM gauge fields propagate in a fifth dimension, masses for the  $W$  and  $Z^0$  bosons can be generated via non-trivial boundary conditions placed on the five-dimensional wavefunctions [3, 4, 5, 6]. Since the need for scalar doublets is eliminated in such scenarios, these models have been aptly dubbed Higgsless models. The result of allowing the SM gauge fields to propagate in the bulk, however, is towers of physical, massive vector gauge bosons (VGBs), the lightest of which are identified with the SM  $W$  and  $Z^0$  bosons. The heavier Kaluza-Klein (KK) modes, which have the  $SU(2) \times U(1)$  quantum numbers of the SM  $W$  and  $Z^0$ , play an important role in longitudinal VGB scattering. In the SM without a Higgs boson, the scattering amplitudes for these processes typically violate unitarity around  $\sim 1.5 \text{ TeV}$  [7]. The exchange of light Higgs bosons, however, cancels the unitarity-violating terms and ensures perturbativity of the theory up to high scales. In extra-dimensional Higgsless models, the exchange of the heavier KK gauge bosons plays the role of the Higgs boson and cancels the dominant unitarity-violating terms [3]. As a result, the scale of unitarity violation can be pushed to the  $\sim 5\text{--}10 \text{ TeV}$  range.

The main drawback of extra-dimensional models is that they are non-renormalizable and, thus, must be viewed as effective theories up to some cutoff scale above which new physics must take over. An extremely efficient and convenient way of studying the phenomenology of five-dimensional effective theories in the context of four-dimensional gauge theories is that of deconstruction [8, 9]. Deconstructed models possess extended gauge symmetries which approximate the fifth dimension, but can be studied in the simplified language of coupled non-linear sigma models (nls) [10, 11, 12]. In fact, this method allows one to effectively separate the perturbatively calculable contributions to low-energy observables from the strongly-coupled contributions due to physics above . The former arise from the new weakly-coupled gauge states, while the latter can be parameterized by adding higher-dimension operators [10, 11, 12, 13, 14, 15].

The phenomenology of deconstructed Higgsless models has been well-studied [14, 16, 17, 18, 19, 20, 21]. Recently, however, the simplest version of these types of models, which involves only three "sites" [14, 16, 22], has received much attention and been shown to be capable of approximating much of the interesting phenomenology associated with extra-dimensional models and more complicated deconstructed Higgsless models [4, 23, 24, 25, 26, 27, 28]. Once EW SB occurs in this model, the gauge sector consists of a massless photon, two relatively light massive VGBs which are identified with the SM  $W$  and  $Z$  gauge bosons, as well as two new heavy VGBs which we denote as  $W^0$  and  $Z^0$ . The exchange of these heavier states in longitudinal VGB scattering can delay unitarity violation up to higher scales [16].

Given the prominent role that the heavier VGBs play in the extra-dimensional and deconstructed Higgsless scenarios, it is important to assess their effects on electroweak precision observables, namely the oblique parameters ( $S$ ;  $T$  and  $U$ ) [29]. These parameters are defined in terms of the SM gauge boson self-energies,  $\Pi_{ij}(q^2)$ , where  $(ij) = (WW); (ZZ); (\gamma\gamma)$  and  $(Z\gamma)$ , and  $q$  is the momentum carried by the external gauge bosons. Generically, the one-loop contributions to the  $\Pi_{ij}$  can be split into four separate classes depending on the particles circulating in the loops: namely, those involving (i) only fermions, (ii) only scalars, (iii) a mixture of scalars and gauge bosons and (iv) only gauge bosons. Due to gauge invariance, class (i) and the sum of classes (ii) and (iii) are independent of the  $R$  gauge used in the calculation. However, class (iv), i.e. contributions to the two-point functions from loops of gauge bosons, are  $R$  gauge-dependent. This was shown explicitly for the case

of one-loop contributions from SM gauge bosons in Ref. [30]. In that paper, the authors showed that in a general  $R_\xi$  gauge the gauge boson self-energies depend non-trivially on the gauge parameter(s)  $\xi_i$  ( $i = W, Z, \dots$ ). These dependences carry over into the calculation of the oblique parameters resulting in gauge-dependent expressions for  $S, T$  and  $U$  [31]. However, in a series of subsequent papers, it was shown that by isolating the gauge-dependent terms from other one-loop corrections (i.e. vertex and box corrections) and combining these with the self-energy expressions derived from the two-point functions, it is possible to define gauge-invariant forms of the self-energies and, thus, obtain gauge-invariant expressions for the oblique parameters [30, 31, 32, 33]. This method of extracting gauge-invariant Green's functions from scattering amplitudes is known as the Pinch Technique (PT) [34, 35, 36, 37].

In this paper, we generalize the results of Refs. [30, 31, 32, 33] to calculate the one-loop, chiral logarithmic corrections to the oblique parameters in extra-dimensional and deconstructed Higgsless models. In our calculation of the PT self-energies, we employ the unitary gauge ( $\xi = 1$ ) to define the massive VGB propagators. The attractive feature of this choice is that unphysical states (i.e. Goldstone bosons, ghosts, etc.) decouple and thus the number of diagrams is drastically reduced. Green's functions calculated in unitary gauge are individually non-renormalizable in the sense that they contain divergences proportional to higher powers of  $q^2$  which cannot be removed by the usual counterterms. However, when the PT is applied, these non-renormalizable terms cancel in the same manner as the gauge-dependent terms mentioned above [33].

The rest of this paper is organized in the following way. In Section II, we discuss the generic Feynman rules used in our calculation. We also describe in some detail the three-site Higgsless model to which we will apply our results in the following sections. Section III contains a general discussion on the Pinch Technique and its use within the unitary gauge. In Sections IV and V, we calculate the one-loop corrections needed to construct the PT self-energies in terms of generic couplings. These corrections are then assembled in Section VI where we explicitly show how to construct the PT gauge boson self-energies. Using these expressions, we calculate the leading chiral-logarithmic corrections to the  $S$  and  $T$  parameters in the three-site model in Section VII. Finally, in Section VIII, we conclude.

## II. THE MODEL(S)

Our results apply to a wide class of Higgsless models in extra-dimensional and deconstructed theories. We begin this section by outlining the types of models for which our calculation is valid. After defining the generic Feynman rules used in our calculation, we discuss the three site Higgsless model in detail and show how it fits within the framework described below.

First, assume that the model has an extended gauge symmetry of the form :

$$SU(2) \times SU(2)^N \times U(1); \quad (1)$$

where the  $U(1)$  is gauged as the  $T_3$  component of a global  $SU(2)$  and the effective four-dimensional Lagrangian for the gauge kinetic terms is:

$$L_G = -\frac{1}{4} B_{\mu\nu} B^{\mu\nu} - \frac{1}{4} \sum_{i=1}^{N+1} W_{\mu\nu}^a W^{\mu\nu a}_i; \quad (2)$$

This gauge structure has been implemented in both extra-dimensional models (where  $N = 1$ ) [4, 5, 6, 38, 39, 40, 41, 42, 43, 44, 45, 46, 47, 48, 49, 50, 51, 52, 53, 54, 55, 56, 57, 58] as well as deconstructed versions ( $N = 1; \dots; 1$ ) [14, 15, 16, 19, 20, 21, 22, 26, 28, 59, 60, 61, 62, 63, 64]. Once EW SB occurs, mixing in both the charged and neutral sectors results in a physical spectrum consisting of a massless photon and "towers" of charged and neutral VGBs. In terms of the mass eigenstates, the gauge fields can be written:

$$W_{\mu}^i = \sum_{n=1}^{N+1} a_{in} W_{(n)}^i; \quad (3)$$

$$B_{\mu} = b_{00} + \sum_{n=1}^{N+1} b_{0n} Z_{(n)}; \quad (4)$$

$$W_{3\mu} = b_{40} + \sum_{n=1}^{N+1} b_{4n} Z_{(n)}; \quad (5)$$

where  $W_{(n)}$  and  $Z_{(n)}$  represent the mass eigenstates, the lightest of which are identified with the SM  $W$  and  $Z$ . In extra-dimensional models, the above expansions would realistically involve infinite towers of massive states; however, in writing Eqs. (3)–(5), we have assumed that only the lightest (i.e., SM-like) and next-to-lightest gauge bosons are important for the phenomenology attainable at present and near-future collider experiments [65]. In general,

the mixing angles  $a_{ij}$  and  $b_{ij}$  can be written in terms of the gauge couplings and the mass eigenvalues and are model-dependent. Inserting Eqs. (3)–(5) into the kinetic energy terms for the SU (2) gauge fields in Eq. (2) generates 3-point and 4-point interactions between the mass eigenstates. The overall couplings for these interactions are functions of the SU (2) gauge couplings and the mixing angles  $a_{ij}$  and  $b_{ij}$ .

Next, we consider the couplings of the fermions to the gauge fields. Assuming the SU (2) gauge fields couple only to left-handed fermions while the U (1) couples to both left- and right-handed fermions, we take as the effective Lagrangian:

$$\begin{aligned} \mathcal{L}_f^{\text{eff}} = & \sum_{n=1}^{N+1} \sum_{i,j} \frac{g_{ijW_n}}{2} \bar{\psi}_i (1 - \gamma_5) \psi_j W_n; + \text{h.c.} \\ & \sum_{n=1}^{N+1} \sum_i \left[ g_{iV_j^0} \bar{\psi}_i \gamma_\mu \psi_i - g_{V_i}^{(V_n^0)} + g_{A_i}^{(V_n^0)} \gamma_5 \right] \bar{\psi}_i V_n^0; \end{aligned} \quad (6)$$

where  $W_n$  and  $V_n^0$  represent the mass eigenstates. Again, the overall couplings  $g_{ijW_n}$  and  $g_{iV_n^0}$ , as well as the coefficients  $g_{V_i}^{(V_n^0)}$  and  $g_{A_i}^{(V_n^0)}$ , are functions of the gauge couplings as well as the mixing angles  $a_{ij}$  and  $b_{ij}$ . Note that electromagnetic gauge invariance requires:

$$\begin{aligned} g_{ff} g_{V_f}^{(\ )} &= e Q_f; \\ g_{ff} g_{A_f}^{(\ )} &= 0; \end{aligned} \quad (7)$$

where  $Q_f$  is the fermion's charge in units of the electron charge  $e$ .

In the following sections, we present our results in terms of generic 3- and 4-point gauge boson couplings, as well as generic fermion-gauge boson couplings. By taking this approach, our results are applicable to any model which fits within the framework outlined above. The Feynman rules used in our calculation are shown in Fig. 1. In these figures, the momenta of the gauge bosons are always defined to be incoming such that the kinematic structures  $V_{3V}$  and  $V_{4V}^i$  take the form:

$$V_{3V} (p; p_+; p_0) = (p_- p_+) g + (p_+ p_0) g + (p_0 p_-) g; \quad (8)$$

$$V_{4V}^i = 2g g + g g + g g; \quad (9)$$

Lastly, the massive gauge boson propagator is defined in terms of the kinematic structure  $G(q; M_V)$  which, in unitary gauge, is given by:

$$G(q; M_V) = g \frac{q_\mu q_\nu}{M_V^2}; \quad (10)$$

$$\begin{aligned}
& \begin{array}{c} V_\mu^-(p_-) \\ \diagup \\ V_\nu^+(p_+) \\ \diagdown \\ V_\lambda^0(p_0) \end{array} = -i g_{V^-V^+V^0} V_{3V}^{\mu\nu\lambda}(p_-, p_+, p_0) \\
\\
& \begin{array}{c} V_\mu^0 \\ \diagup \\ V_\lambda^- \\ \diagdown \\ V_\rho^+ \end{array} = -i g_{V^0V^0V^-V^+} V_{4V}^{\mu\nu,\lambda\rho}; \quad \begin{array}{c} V_\mu^+ \\ \diagup \\ V_\lambda'^- \\ \diagdown \\ V_\rho'^- \end{array} = -i g_{V^+V^+V'^-V'^-} V_{4V}^{\mu\nu,\lambda\rho} \\
\\
& \begin{array}{c} V_\mu^\pm \\ \diagup \\ f' \\ \diagdown \\ f \end{array} = -\frac{i}{2\sqrt{2}} g_{ff'V^\pm} \gamma_\mu (1 - \gamma_5) \\
\\
& \begin{array}{c} V_\mu^0 \\ \diagup \\ f \\ \diagdown \\ f \end{array} = -i g_{ffV^0} \gamma_\mu [g_{V_f}^{(V^0)} + g_{A_f}^{(V^0)} \gamma_5] \\
\\
& \begin{array}{c} V \\ \mu \xrightarrow{q} \nu \end{array} = \frac{-i}{q^2 - M_V^2} G_{\mu\nu}(q; M_V)
\end{aligned}$$

FIG . 1: Generic Feynman rules used in our calculation. All kinematic functions and coupling constants are defined in the text.

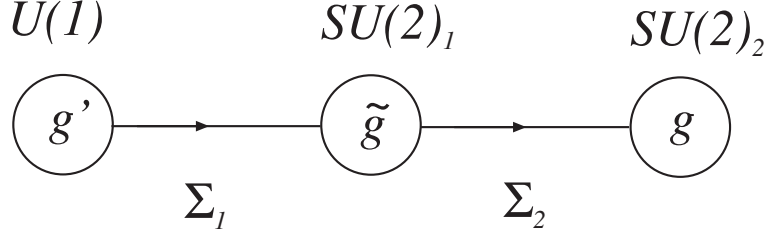


FIG. 2: Moose diagram for the three site model (from Ref. [16]). The local gauge symmetry  $SU(2)_1 \times SU(2)_2 \times U(1)$  is gauged as the subgroup of a global  $SU(2)^3$  symmetry.

where  $M_V$  is the mass of the propagating gauge boson.

We turn now to the three site Higgsless model which is a prototypical example of the models outlined above.

#### A. The Three Site Higgsless Model

The three site Higgsless model [14, 16, 22] is a nlm based on the global  $SU(2)^3 \rightarrow SU(2)$  symmetry breaking pattern, where the remaining  $SU(2)$  plays the role of the custodial symmetry. The gauged sub-group is  $SU(2)_1 \times SU(2)_2 \times U(1)$  and the symmetry breaking to the SM  $SU(2)_L \times U(1)_Y$  is achieved by two bifundamental fields as depicted in the "moose" diagram shown in Fig. 2.

The nlm fields  $\chi_{1,2}$  consist of two  $SU(2)$  triplets:

$$\chi_1 = \exp \frac{2i \chi_1^a T^a}{f_1} ; \quad \chi_2 = \exp \frac{2i \chi_2^a T^a}{f_2} ; \quad (11)$$

which are coupled to the gauge fields through the covariant derivatives:

$$D_{\chi_1} = \partial_{\chi_1} - ig^0 T^3 B_{\chi_1} + ig_1 T^a W_{1,\chi_1}^a ; \quad (12)$$

$$D_{\chi_2} = \partial_{\chi_2} - ig_2 T^a W_{2,\chi_2}^a + ig_2 T^a W_{2,\chi_2}^a ; \quad (13)$$

where  $g^0$  is the gauge coupling of the  $U(1)$ , while  $g$  and  $g$  are the gauge couplings of  $SU(2)_1$  and  $SU(2)_2$ , respectively.

The effective Lagrangian for the three site model can be written as an expansion in derivatives (momenta). At lowest order (dimension-2), the relevant terms which obey the



custodial symmetry are:

$$L_2 = \sum_{i=1}^{X^2} \frac{f_i^2}{4} \text{Tr} [D_i (D_i)^\dagger] - \frac{1}{4} \sum_{i=1}^{X^2} W_i^a W_i^a - \frac{1}{4} B B : \quad (14)$$

In addition to these terms, there is one additional dimension-2 operator which violates the custodial symmetry:

$$L_2^0 = c_{(2)} f_1^2 \text{Tr} [T^3 (D_1) T^3] \text{Tr} [T^3 (D_1) T^3]; \quad (15)$$

as well as dimension-4 operators that respect the symmetries of the theory [15]:

$$\begin{aligned} L_4 = & c_{(1)1} \text{Tr} [W_2; W_1 T^3 B] + c_{(2)1} \text{Tr} [W_1; T^3 B] \\ & 2i c_{(1)2} \text{Tr} [(D_2)^\dagger (D_2) W_1] - 2i c_{(2)2} \text{Tr} [(D_1)^\dagger (D_1) T^3 B] \\ & + \sum_{i=1}^{X^2} 2i c_{(i)3} \text{Tr} [W_i (D_i) (D_i)^\dagger] + c_{(i)4} \text{Tr} [(D_i) (D_i)^\dagger] \text{Tr} [(D_i) (D_i)^\dagger] \\ & + c_{(i)5} \text{Tr} [(D_i) (D_i)^\dagger] \text{Tr} [(D_i) (D_i)^\dagger] : \end{aligned} \quad (16)$$

The coefficients of these terms act as counterterms for the divergences which appear at one-loop order and serve to parameterize the effects of unknown high-scale physics [10, 11, 12, 13, 14, 15]. As we will discuss later, the  $c_{(2)}$  coefficient contributes to the  $T$  parameter while the  $c_{(1)1}$  coefficients are relevant to the  $S$  parameter.

In unitary gauge ( $\xi \rightarrow \infty$ ), the kinetic energy terms for the fields in Eq. (14) only serve to give mass to the various gauge fields. Diagonalizing the resulting charged- and neutral-sector mass matrices, one finds that the spectrum consists of a (massless) photon, relatively light charged and neutral gauge bosons ( $W$  and  $Z$ ), as well as heavy charged and neutral gauge bosons ( $W^0$  and  $Z^0$ ). At this point, there are five free parameters in the model:  $g; g^0; g; f_1$  and  $f_2$ . For the purposes of our calculation, we find it useful to follow Ref. [16] and exchange these parameters for the masses of the light VGBs ( $M_W$  and  $M_Z$ ), the masses of the heavy VGBs ( $M_{W^0}$  and  $M_{Z^0}$ ) and the electromagnetic charge  $e$ . The latter of which is defined in this model to be:

$$\frac{1}{e^2} = \frac{1}{g^2} + \frac{1}{g^2} + \frac{1}{g^2} : \quad (17)$$

The gauge elds can be expanded in terms of the mass eigenstates. The charged elds can be written as:

$$W_1 = a_{11}W^0 + a_{12}W^-; \quad (18)$$

$$W_2 = a_{21}W^0 + a_{22}W^-; \quad (19)$$

while the neutral elds are given by:

$$B = b_{00} + b_{01}Z^0 + b_{02}Z; \quad (20)$$

$$W_1^3 = b_{10} + b_{11}Z^0 + b_{12}Z; \quad (21)$$

$$W_2^3 = b_{20} + b_{21}Z^0 + b_{22}Z; \quad (22)$$

Precise formulae for the gauge couplings, the decay constants ( $f_1$  and  $f_2$ ) and the mixing angles ( $a_{ij}$  and  $b_{ij}$ ) in terms of the masses of the gauge bosons can be found in Appendix B.

We can now make connection with the generic Feynman rules for the 3- and 4-gauge boson interactions shown in Fig. 1. Inserting Eqs. (18)–(22) into the gauge kinetic terms in Eq. (14), we find that the 3- and 4-point couplings relevant to the calculation of the S and T parameters are given by:

$$g_{W^-W^+V_i^0} = g a_{22}^2 b_{2i} + g a_{12}^2 b_{1i}; \quad (23)$$

$$g_{W^-W^0V_i^0} = g a_{21} a_{22} b_{2i} + g a_{11} a_{12} b_{1i}; \quad (24)$$

$$g_{W^0W^0V_i^0} = g a_{21}^2 b_{2i} + g a_{11}^2 b_{1i}; \quad (25)$$

and:

$$g_{V_i^0V_j^0W^-W^+} = g^2 a_{22}^2 b_{2i} b_{2j} + g^2 a_{12}^2 b_{1i} b_{1j}; \quad (26)$$

$$g_{V_i^0V_j^0W^0W^0} = g^2 a_{21}^2 b_{2i} b_{2j} + g^2 a_{11}^2 b_{1i} b_{1j}; \quad (27)$$

$$g_{W^-W^+W^-W^0} = g^2 a_{21}^2 a_{22}^2 + g^2 a_{11}^2 a_{12}^2; \quad (28)$$

$$g_{W^-W^+W^-W^-} = g^2 a_{22}^4 + g^2 a_{12}^4; \quad (29)$$

where  $(V_0^0; V_1^0; V_2^0) = (\gamma; Z^0; Z)$ .

Next, we consider the couplings of the fermions to the gauge elds. We assume only direct couplings of the left-handed fermions to  $SU(2)_2$  while the left- and right-handed fermions couple to the  $U(1)$  with charges  $Y_L$  and  $Y_R$ , respectively. In the language of deconstruction, we have "localized" the fermions on the first and third sites. This will lead

to an (unacceptably) large tree-level contribution to the S parameter [14, 16, 22]. However, this large contribution can be reduced (or eliminated altogether) by allowing the fermions to have a small (but non-zero) coupling to the "middle" SU(2) of Fig. 2 [22, 63]. Since we are only interested in illustrating how to apply our calculation to a particular model, we will keep the fermions localized at the first and third sites. Generalizing our results to the case of "delocalized" fermions is straightforward.

The effective Lagrangian describing the coupling of fermions to gauge bosons is then given by [16]:

$$\mathcal{L}_f = g^0 (Y_L P_L + Y_R P_R) B + g T^a W^a_2 P_L ; \quad (30)$$

where  $P_{L,R}$  are projection operators:

$$P_{L,R} = \frac{1}{2}(1 \pm \gamma_5) ; \quad (31)$$

Expressing the gauge fields in terms of the mass eigenstates using Eqs. (20) and (22), we can identify the couplings and coefficients used in our generic Feynman rules. For example, the couplings for the charged-current interactions are given by:

$$g_{ffW^\pm} = g a_{21} ; \quad (32)$$

$$g_{ffW^0} = g a_{22} ; \quad (33)$$

Next, the expressions for the neutral-current couplings and coefficients can be simplified by making the identification  $Y_R = Y_L + T_f^3 = Q_f$ . In fact, we find:

$$g_{ffV_i^0} = g b_{2i} - g b_{0i} ; \quad (34)$$

and:

$$g_{V_f}^{(V_i^0)} = \frac{1}{2} T_f^3 + \frac{g b_{0i}}{(g b_{2i} - g b_{0i})} Q_f ; \quad (35)$$

$$g_{A_f}^{(V_i^0)} = \frac{1}{2} T_f^3 ; \quad (36)$$

Having now specified the types of models we are interested in, let us discuss the pinch technique in more detail as well as its application to models with extra dimensions and/or extended gauge symmetries.

### III. UNITARY GAUGE AND THE PT

As mentioned in the Introduction, vector-bosonic loop corrections to the VGB self-energies suffer from two troublesome issues: (i) the naive expressions are non-trivially dependent on the particular  $R$  gauge used and (ii) use of the unitary gauge ( $R \rightarrow 1$ ) results in non-renormalizable terms. The first issue has been studied in detail in Refs. [30, 31, 32, 33]. In this paper, we employ the unitary gauge in order to reduce the number of diagrams. Therefore, let us discuss the second issue and its resolution in more detail.

While the unitary gauge is known to result in renormalizable  $S$ -matrix elements, Green's functions calculated in this gauge are individually non-renormalizable. These terms are non-renormalizable in the sense that they cannot be removed by the usual mass- and field-renormalization counterterms. To see how this arises, consider the form of the massive VGB propagator in unitary gauge:

$$D_{ij} = \frac{i}{q^2 - M_i^2} g_{ij} - \frac{q_i q_j}{M_i^2} : \quad (37)$$

The problem arises in the limit  $q^2 \rightarrow 1$  where  $D_{ij} \rightarrow 1$ . In this limit, one-loop amplitudes containing one or more propagators of the form in Eq. (37) become highly divergent. In particular, if dimensional regularization is applied, this divergent behavior manifests itself in poles proportional to higher powers of the external momentum-squared ( $q^2$ ) [33]. For example, two-point functions calculated in unitary gauge contain poles proportional to  $q^4$  and  $q^6$ .

The Pinch Technique supplies a solution to both the gauge-dependence and the appearance of the  $q^4$  and  $q^6$  terms via a systematic algorithm which leads to the rearrangement of one-loop Feynman graphs contributing to a gauge-invariant and renormalizable amplitude [34, 35, 36, 37]. The end results of the rearrangement are individually gauge-independent propagator-, vertex- and box-like structures which are void of any higher powers of  $q^2$ . In other words, propagator-like or "pinch" terms coming from vertex and box corrections are isolated in a systematic manner and added to the self-energies. These pinch pieces carry the exact gauge-dependent and non-renormalizable terms needed to cancel those of the two-point functions. Finally, to construct gauge-invariant expressions for the oblique parameters at one-loop, one needs only replace the various  $\Pi_{ij}$  calculated from two-point diagrams with their PT counterparts,  $\Pi_{ij}^{PT}$  [31]. In the following sections, we will demonstrate how to

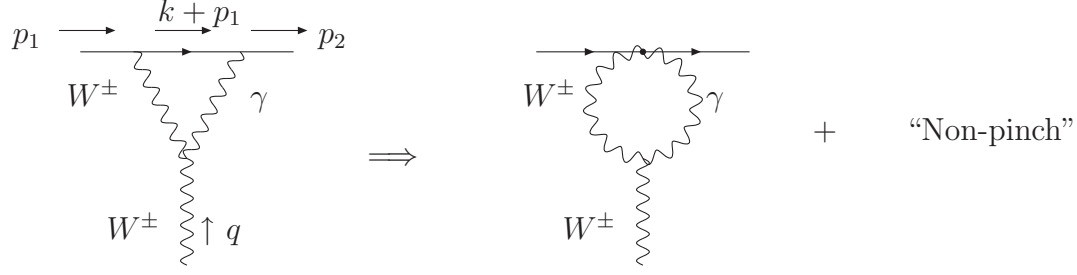


FIG. 3: Schematic example of the extraction of pinch pieces from vertex corrections.

construct the PT self-energies in models with additional, massive gauge bosons.

Before moving on to our results, though, let us first give a simple example of how the pinch terms are isolated. Consider the vertex diagram shown on the left side of Fig. 3 where the external and internal fermions are considered to be massless. When the  $W$  propagator (with loop momentum  $k$ ) is contracted with the  $Wff^0$  vertex, a term arises of the form :

$$\begin{aligned}
 A_V &= \int \frac{d^n k}{(2\pi)^n} u(p_2) \left( \cancel{(\not{k} + \not{p}_1)} \right) u(p_1) \frac{1}{(k^2 - M_W^2)(k + p_1)^2(k - q)^2} \\
 &= \int \frac{d^n k}{(2\pi)^n} u(p_2) \left( \not{k} \right) (\not{k} + \not{p}_1) \cancel{(\not{p}_1)} u(p_1) \frac{1}{(k^2 - M_W^2)(k + p_1)^2(k - q)^2} \\
 &= \int \frac{d^n k}{(2\pi)^n} u(p_2) (\not{k})^2 \cancel{p} u(p_1) \frac{1}{(k^2 - M_W^2)(k + p_1)^2(k - q)^2} + \dots : \quad (38)
 \end{aligned}$$

In the second line, we have written the second factor of  $\cancel{k}$  in terms of adjacent, inverse fermion propagators. Canceling the factor of  $(k + p_1)^2$  in the numerator and denominator, we see that the first term in the third line resembles a correction to the  $W$  propagator, i.e. it is propagator-like, and can be represented schematically as shown on the right side of Fig. 3. This pinch term (along with others coming from other vertex and box corrections) is then combined with the loop-corrected two-point function to construct the self-energy for the  $W$  boson.

#### IV. ONE-LOOP CORRECTIONS TO THE NEUTRAL CURRENTS

In this section, we outline the calculation of the one-loop corrections needed to construct the self-energies for the neutral gauge bosons using the Pinch Technique [30, 32]. We write all amplitudes in terms of the generic couplings defined in Fig. 1 and reduce all tensor

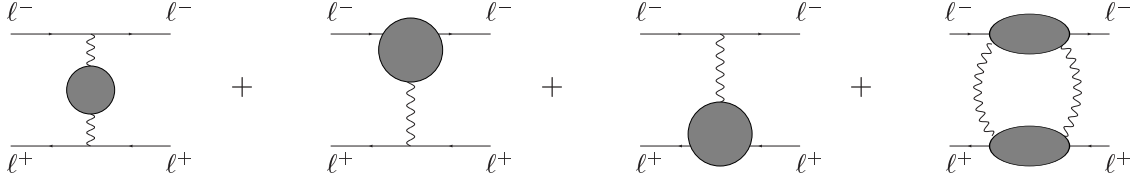


FIG. 4: One-loop corrections to t-channel  $\ell^-\ell^+$  scattering. From left to right, the corrections consist of one-loop corrections to the gauge boson propagator, corrections to the  $V^0\ell\ell$  vertices and box corrections.

$$\begin{array}{c} Z, \gamma \\ \xrightarrow{q} \end{array} \text{bubble} \begin{array}{c} Z, \gamma \\ \xrightarrow{q} \end{array} = \sum_{i,j} \begin{array}{c} V_j^+ \\ \text{wavy line} \\ V_i^- \\ (S_{1,ij}^{NC}) \end{array} + \sum_i \begin{array}{c} V_i^\pm \\ \text{wavy line} \\ V_i^\pm \\ (S_{2,i}^{NC}) \end{array}$$

FIG. 5: General corrections to the two-point functions of the neutral gauge bosons.

integrals to the usual Passarino-Veltman (P-V) tensor integral coefficients [66] and scalar integrals defined in Appendix A.

The PT selfenergies for the neutral VGBs are calculated in the context of four-fermion scattering, in particular  $\ell^-\ell^+ \rightarrow \ell^-\ell^+$ , with all external (and internal) fermions considered to be massless<sup>1</sup>. The one-loop corrections are shown schematically in Fig. 4. In the following, we calculate the corrections to the gauge boson propagators, as well as the pinch pieces from both vertex and box corrections.

#### A. Corrections to the Gauge Boson Propagators

The one-loop corrections to the neutral gauge boson propagators are shown in Fig. 5. In terms of the amplitudes of these diagrams, the transverse two-point functions for the SM

<sup>1</sup> It is straightforward to show that the results given below are independent of the particular choice of four-fermion scattering process

neutral gauge bosons can be constructed as:

$$i_{mn}(q^2)g = i \sum_{i,j}^X S_{1ij}^{NC;} + \sum_i^X S_{2i}^{NC;} ; \quad (39)$$

where  $(mn) = (\gamma\gamma); (ZZ)$  or  $(Z\gamma)$ . The structures of the individual amplitudes take the form s:

$$S_{1ij}^{NC;} = g_{V_i V_j}^2 (Z) C_S^{(0)} + C_S^{(2)} q^2 + C_S^{(4)} q^4 g ; \quad (40)$$

$$S_2^{NC;} = g_{(ZZ)V_i V_i^+} \left[ \frac{9}{2} + \frac{15}{4} A_0(M_i) \right] g ; \quad (41)$$

where:

$$\begin{aligned} C_S^{(0)} = & 10 + \frac{M_i^2}{M_j^2} + \frac{M_j^2}{M_i^2} - 8 B_{22}(q^2; M_i, M_j) + \frac{M_i^2 + M_j^2}{M_j^2} \frac{M_i^4}{M_j^2} B_0(q^2; M_i, M_j) \\ & + \frac{1}{4} \frac{M_j^2}{M_i^2} + \frac{1}{8} A_0(M_i) + \frac{1}{4} \frac{M_i^2}{M_j^2} + \frac{1}{8} A_0(M_j) ; \end{aligned} \quad (42)$$

$$\begin{aligned} C_S^{(2)} = & 2 \left[ \frac{1}{M_i^2} + \frac{1}{M_j^2} \right] B_{22}(q^2; M_i, M_j) + 2 \left[ 2 + \frac{M_i^2}{M_j^2} + \frac{M_j^2}{M_i^2} \right] B_0(q^2; M_i, M_j) \\ & + \frac{1}{M_i^2} A_0(M_i) + \frac{1}{M_j^2} A_0(M_j) ; \end{aligned} \quad (43)$$

$$C_S^{(4)} = \frac{1}{M_i^2 M_j^2} B_{22}(q^2; M_i, M_j) - (M_i^2 + M_j^2) B_0(q^2; M_i, M_j) ; \quad (44)$$

In the above and the following,  $A_0$  and  $B_0$  represent the one- and two-point scalar integrals, respectively, while the  $B_{ij}$ 's represent the P-V tensor integral coefficients [66] (see Appendix A).

## B. Pinch Contributions from Vertex Corrections

The one-loop vertex corrections for the neutral current are shown in Fig. 6. Note that we have included the external leg corrections in addition to the traditional vertex corrections. The pinch contributions to the total amplitude from these vertex corrections take the form :

$$\begin{aligned} A_{V; (Z)}^{\text{pinch}} = & fV_{(Z)} g [u(p_i) - (1 - \gamma_5) u(p_i)] \\ & fV_{(Z)} g \bar{w} ; \end{aligned} \quad (45)$$

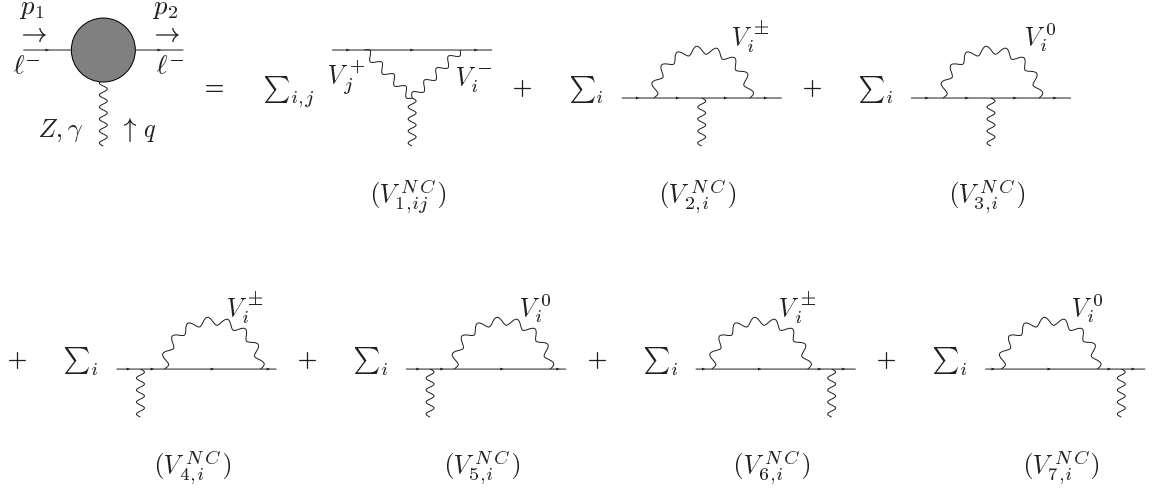


FIG. 6: General one-loop corrections to the neutral gauge-boson-fermion vertices and the external legs which give rise to pinch contributions.

where  $\text{fv}_{(\mathbb{Z})g}$  represents the sum of the pinch contributions calculated from the diagrams shown in Fig. 6 and  $\mathbf{w}$  is the current associated with the SM-like  $W$ . In applying the PT to the neutral currents, we find it useful to rewrite  $\mathbf{w}$  in terms of the currents associated with the SM-like  $Z$  and photon. For example, using Eqs. (34)–(36), this structure in the three site model can be rewritten as:

$$\begin{aligned}
\mathbf{w} \cdot \mathbf{u}(\mathbf{p}) - (1 - \xi_5) \mathbf{u}(\mathbf{p}_i) &= \frac{2}{T_f^3} \mathbf{u}(\mathbf{p}_j) - \frac{1}{2} T_f^3 + \frac{g^0 b_{02}}{(g b_{22} - g^0 b_{02})} Q_f \\
&\quad - \frac{g^0 b_{02}}{(g b_{22} - g^0 b_{02})} Q_f - \frac{1}{2} T_f^3 - \xi_5 \mathbf{u}(\mathbf{p}_i) \\
&= \frac{2}{T_f^3} \mathbf{u}(\mathbf{p}_j) - (g_{V_f}^{(Z)} + g_{A_f}^{(Z)} \xi_5) + \frac{g^0 b_{02}}{(g b_{22} - g^0 b_{02})} Q_f - \mathbf{u}(\mathbf{p}_i) \\
&\quad - \frac{2}{T_f^3} \mathbf{z} + \frac{g^0 b_{02}}{(g b_{22} - g^0 b_{02})} Q_f \quad ; \quad (46)
\end{aligned}$$



where we have defined the currents associated with the SM  $Z$  and photon respectively as:

$$j_Z = \bar{u}(p_j) (g_{V_f}^{(Z)} + g_{A_f}^{(Z)}) u(p_i); \quad (47)$$

$$= \bar{u}(p_j) - u(p_i): \quad (48)$$

Using the Feynman rules defined in Fig. 1 and reducing all amplitudes to P-V tensor coefficients and scalar integrals, we find that the pinch pieces from the individual diagrams shown in Fig. 6 are given by:

$$fV_{1;ij}^{NC} g = g_{V_i} g_{V_j} g_{(Z)V_j^+ V_i} [C_V^{(0)} + C_V^{(2)} q^2] \quad (49)$$

$$fV_{2;i}^{NC} g = g_{V_i}^2 g_{(Z)} [g_V^{(iZ)} - g_A^{(iZ)}] \frac{A_0(M_i)}{M_i^2} \quad (50)$$

$$\begin{aligned} fV_{3;i}^{NC} g &= g_{V_i}^2 g_{(Z)} \frac{A_0(M_i)}{M_i^2} u(p_2) (2g_V^{(V^0)} g_A^{(V^0)} g_A^{(iZ)} + (g_V^{(V^0)})^2 g_V^{(iZ)} + (g_A^{(V^0)})^2 g_V^{(iZ)}) \\ &\quad + (2g_V^{(V^0)} g_A^{(V^0)} g_V^{(iZ)} + (g_V^{(V^0)})^2 g_A^{(iZ)} + (g_A^{(V^0)})^2 g_A^{(iZ)}) u(p_1) \end{aligned} \quad (51)$$

$$fV_{4;i}^{NC} g = \frac{g_{V_i}^2 g_{(Z)}}{2} (g_V^{(iZ)} - g_A^{(iZ)}) \frac{A_0(M_i)}{M_i^2} \quad (52)$$

$$fV_{5;i}^{NC} g = \frac{1}{2} fV_{3;i}^{NC} g \quad (53)$$

$$fV_{6;i}^{NC} g = fV_{4;i}^{NC} g \quad (54)$$

$$fV_{7;i}^{NC} g = fV_{5;i}^{NC} g = \frac{1}{2} fV_{3;i}^{NC} g; \quad (55)$$

where:

$$C_V^{(0)} = (3+2) \frac{1}{M_i^2} + \frac{1}{M_j^2} B_{22}(q^2; M_i; M_j) + 2B_0(q^2; M_i; M_j) \quad (56)$$

$$\begin{aligned} C_V^{(2)} &= \frac{1}{M_j^2} B_0(q^2; M_i; M_j) - \frac{2}{M_i^2} B_{11}(q^2; M_i; M_j) - \left( \frac{1}{M_i^2} + \frac{1}{M_j^2} \right) B_{21}(q^2; M_i; M_j) \\ &\quad - \frac{1}{M_i^2 M_j^2} B_{22}(q^2; M_i; M_j) : \end{aligned} \quad (57)$$

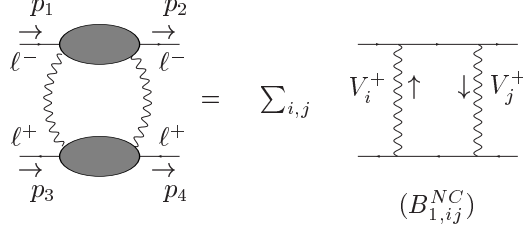


FIG . 7: General one-loop box corrections from charged VGBs which contain pinch contributions.

Thus, we immediately see that the pinch pieces from the vertex corrections and external leg corrections containing a virtual, neutral gauge boson ( $V^0$ ) cancel amongst themselves, i.e.:

$$fV_{3;i}^{NC}g + fV_{5;i}^{NC}g + fV_{7;i}^{NC}g = 0 : \quad (58)$$

Note that this is true regardless of the exact form of the couplings. Finally, in terms of the above amplitudes, the total pinch contribution from the vertex corrections is given by:

$$fV_{(Z)}g = \sum_{i;j} fV_{1;ij}^{NC}g + \sum_i fV_{2;i}^{NC}g + fV_{4;i}^{NC}g + fV_{6;i}^{NC}g : \quad (59)$$

### C . Pinch Contributions from Box Corrections

The one-loop box diagrams which give rise to pinch contributions are depicted in Fig. 7. The total pinch amplitude arising from these corrections can be written as:

$$A_{B;(Z)}^{pinch} = fB_{(Z)}g_{WW}; \quad (60)$$

where  $fB_{(Z)}g$  represents the sum of the pinch contributions from the box diagrams. Individually, the amplitudes for these diagrams take the compact form :

$$fB_{1;ij}^{NC}g = \frac{g_{V_i}^2 g_{V_j}^2}{M_i^2 M_j^2} B_{22}(q^2; M_i, M_j) - (M_i^2 + M_j^2) B_0(q^2; M_i, M_j) : \quad (61)$$

such that the total pinch contributions from box corrections  $fB_{1;ij}^{NC}g$  is given by:

$$fB_{(Z)}g = \sum_{i;j} fB_{1;ij}^{NC}g : \quad (62)$$

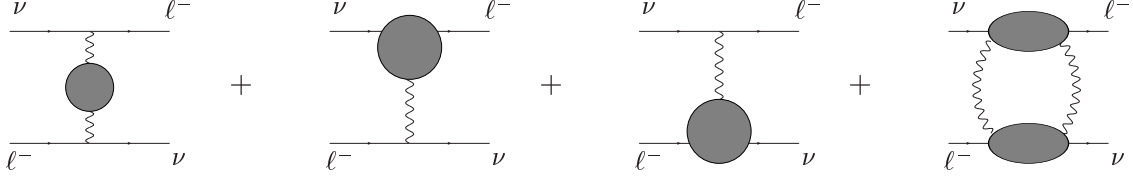


FIG . 8: Schematic depiction of the one-loop corrections to t-channel scattering.

$$\begin{aligned}
 \begin{array}{c} W \\ \rightarrow q \end{array} \text{---} \text{---} \text{---} \begin{array}{c} W \\ \rightarrow q \end{array} &= \sum_i \begin{array}{c} \gamma \\ \text{---} \text{---} \text{---} \\ V_i^\pm \\ (S_{1,i}^{CC}) \end{array} + \sum_{i,j} \begin{array}{c} V_j^0 \\ \text{---} \text{---} \text{---} \\ V_i^\pm \\ (S_{2,ij}^{CC}) \end{array} + \sum_i \begin{array}{c} V_i^\pm \\ \text{---} \text{---} \text{---} \\ (S_{3,i}^{CC}) \end{array} + \sum_i \begin{array}{c} V_i^0 \\ \text{---} \text{---} \text{---} \\ (S_{4,i}^{NC}) \end{array}
 \end{aligned}$$

FIG . 9: General corrections to the two-point functions of the W gauge boson.

## V . ONE-LOOP CORRECTIONS TO THE CHARGED CURRENT

In this section, we calculate the one-loop corrections needed to construct the W boson self-energy using the PT [33]. The loop-corrected amplitudes are again calculated in the context of four-fermion scattering. In particular, we consider the one-loop corrections to  $\ell^+ \ell^- \rightarrow \nu \bar{\nu}$  which are schematically depicted in Fig. 8.

### A . Corrections to the W Boson Propagator

The one-loop corrections to the W boson propagator are shown in Fig. 9. In terms of these diagrams, the transverse two-point function of the W boson is:

$$i_{WW}(q^2)g = i \sum_i S_{1,i}^{CC;} + \sum_{i;j} S_{2,ij}^{CC;} + \sum_i S_{3,i}^{CC;} + \sum_i S_{4,i}^{CC;} : \quad (63)$$

Note that we have distinguished the photon from the other neutral gauge bosons in Fig. 9. Since the photon is massless, the kinematic structures of these diagrams are slightly different than those for massive, neutral gauge bosons. The amplitudes for all of these diagrams take

compact form s:

$$S_{1;i}^{CC}; = g_W^2 V_i^+ K_S^{(0)} + K_S^{(2)} q^2 + K_S^{(4)} q^4 g ; \quad (64)$$

$$S_{2;ij}^{CC}; = g_W^2 V_i^+ V_j^0 C_S^{(0)} + C_S^{(2)} q^2 + C_S^{(4)} q^4 g ; \quad (65)$$

$$S_{3;i}^{CC}; = g_{W^+ V_i^+ W^- V_i} \left( \frac{9}{4} + \frac{15}{8} A_0(M_i) \right) g ; \quad (66)$$

$$S_{4;i}^{CC}; = g_{V_i^0 V_i^0 W^- W^+} \left( \frac{9}{4} + \frac{15}{8} A_0(M_i) \right) g ; \quad (67)$$

where the  $C_S^{(i)}$  coefficients are the same as those in Eqs. (42)–(44) and the  $K_S^{(i)}$  coefficients are given by:

$$K_S^{(0)} = (10 - 8) B_{22}(q^2; M_i; 0) + M_i^2 B_0(q^2; M_i; 0) + \frac{1}{4} + \frac{1}{8} A_0(M_i) ; \quad (68)$$

$$K_S^{(2)} = \frac{2}{M_i^2} B_{22}(q^2; M_i; 0) + 4 B_0(q^2; M_i; 0) + \frac{A_0(M_i)}{M_i^2} ; \quad (69)$$

$$K_S^{(4)} = \frac{1}{M_i^2} B_0(q^2; M_i; 0) : \quad (70)$$

## B . Pinch Contributions from Vertex Corrections

The one-loop vertex corrections which give rise to pinch contributions are shown in Fig. 10. The amplitude structure of these diagrams is very similar to the neutral current amplitudes with the exception of diagrams  $(V_{1;i}^{CC})$  and  $(V_{2;i}^{CC})$ . The pinch contributions from the vertex corrections take the form :

$$A_{V_W}^{pinch} = f V_W g_W ; \quad (71)$$

$$\begin{aligned}
& \text{Diagram 1: } p_1 \rightarrow \nu \xrightarrow{\gamma^*} W^- \xrightarrow{q} \ell^- \leftarrow p_2 \\
& = \sum_i V_{1,i}^{CC} + \sum_{i,j} V_{2,ij}^{CC} + \sum_{i,j} V_{3,ij}^{CC} \\
& + \sum_i V_{4,i}^{CC} + \sum_i V_{5,i}^{CC} + \sum_i V_{6,i}^{CC} \\
& + \sum_i V_{7,i}^{CC} + \sum_i V_{8,i}^{CC} + \sum_i V_{9,i}^{CC}
\end{aligned}$$

FIG. 10: General one-loop corrections to the gauge-boson-fermion vertices and external fermion legs which give rise to pinch contributions.

where  $fV_W g$  is the sum of the pinch contributions from the diagrams in Fig. 10 and  $\Gamma_W$  is defined in Eq. (45). The individual amplitudes which contribute to  $fV_W g$  can be written as:

$$fV_{1;i}^{CC} g = \frac{g_{V_i} g_{V_j} g_W}{2^2} \frac{v_i^+}{2} (g_V^{(1)} q_A^{(1)}) [K_V^{(0)} + K_V^{(2)} q^2]; \quad (72)$$

$$fV_{2;j}^{CC} g = \frac{g_{V_i} g_{V_j} g_W}{2^2} \frac{v_j^0}{2} (g_V^{(V^0)} q_A^{(V^0)}) [C_V^{(0)} + C_V^{(2)} q^2]; \quad (73)$$

$$fV_{3;j}^{CC} g = \frac{g_{V_j} g_{V_i} g_W}{2^2} \frac{v_j^+ v_i^0}{2} (g_V^{(V^0)} q_A^{(V^0)}) [C_V^{(0)} + C_V^{(2)} q^2]; \quad (74)$$

$$fV_{4;i}^{CC} g = \frac{g_{V_i}^2 g_W}{2^2} \frac{1}{2} \frac{A_0(M_i)}{M_i^2}; \quad (75)$$

$$fV_{5;i}^{CC} g = \frac{g_{V_i} g_{V_j} g_W}{2^2} \frac{v_i^0}{2} (g_V^{(V^0)} q_A^{(V^0)}) (g_V^{(V^0)} q_A^{(V^0)}) \frac{A_0(M_i)}{M_i^2}; \quad (76)$$

$$fV_{6;i}^{CC} g = fV_{4;i}^{CC} g; \quad (77)$$

$$fV_{7;i}^{CC} g = \frac{g_{V_i}^2 g_W}{2^2} \frac{1}{2} (g_V^{(V^0)} q_A^{(V^0)})^2 \frac{A_0(M_i)}{M_i^2}; \quad (78)$$

$$fV_{8;i}^{CC} g = fV_{6;i}^{CC} g = fV_{4;i}^{CC} g; \quad (79)$$

$$fV_{9;i}^{CC} g = \frac{g_{V_i}^2 g_W}{2^2} \frac{1}{2} (g_V^{(V^0)} q_A^{(V^0)})^2 \frac{A_0(M_i)}{M_i^2}; \quad (80)$$

where the  $C_V^{(i)}$  coefficients are given by Eqs. (56) and (57) and the  $K_V^{(i)}$  coefficients are given by:

$$K_V^{(0)} = \frac{1}{M_i^2} (3 + 2) B_{22}(q^2; M_i; 0) + 2 B_{00}(q^2; M_i; 0); \quad (81)$$

$$K_V^{(2)} = \frac{1}{M_i^2} B_{00}(q^2; 0; M_i) - B_{21}(q^2; 0; M_i); \quad (82)$$

Finally, the total pinch contribution from the vertex corrections can then be calculated

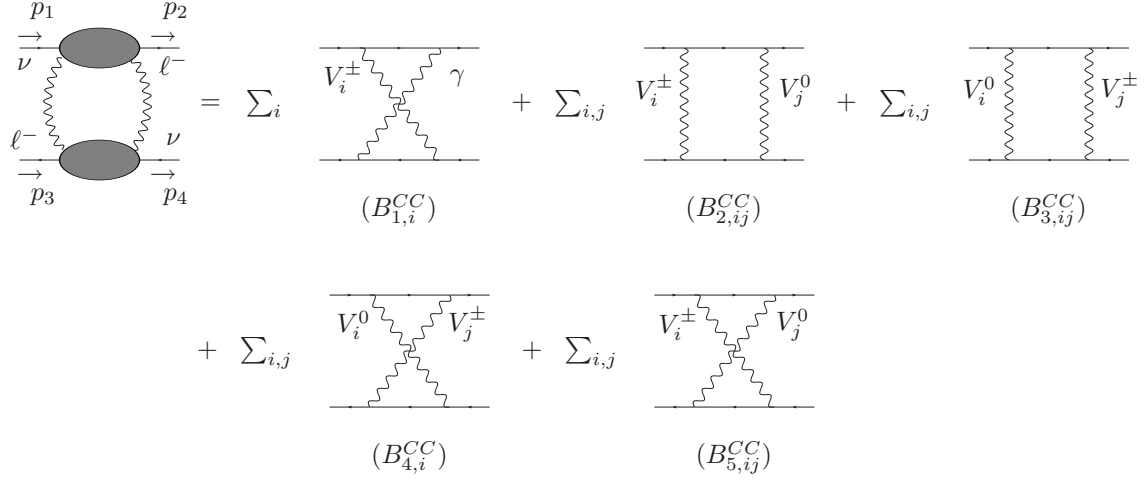


FIG .11: General one-loop box corrections to the charged current process.

by summing the above amplitudes:

$$\begin{aligned}
 fV_W g = & \sum_i fV_{1,i}^{CC} g + fV_{4,i}^{CC} g + fV_{5,i}^{CC} g + fV_{6,i}^{CC} g + fV_{7,i}^{CC} g + fV_{8,i}^{CC} g + fV_{9,i}^{CC} g \\
 & + \sum_{i,j} fV_{2,ij}^{CC} g + fV_{3,ij}^{CC} g : 
 \end{aligned} \tag{83}$$

### C . Pinch Contributions from Box Corrections

The one-loop box corrections which contribute to the  $W$  boson PT self-energy are shown in Fig 11. Extracting the pinch contributions, the amplitude from box corrections takes the form :

$$A_{B,W}^{pinch} = fB_W g_{W-W}; \tag{84}$$

where  $fB_W g$  represents the pinch piece of the total box amplitude. Since the photon only couples to charged fermions, there is only one diagram involving a photon which gives a non-zero contribution to the total pinch amplitude:

$$fB_{1,i}^{CC} g = \frac{g_V^2 g_A^2}{(2-p_i^2)^2} \frac{(g_V^{(i)} g_A^{(i)})^2}{M_i^2} B_0(q_i^2; M_i^2; 0) : \tag{85}$$

The other four diagrams, those which contain a massive neutral gauge boson as well as a massive charged gauge boson, have kinematic structures identical to  $fB_{1,i}^{CC} g$  (Eq. (61)). In

fact, we find:

$$\text{fB}_{2;ij}^{\text{CC}} g = \frac{g_{V_j^0} g_{V_j^0} g_{V_i^0}^2}{(2 - \frac{1}{2})^2} \frac{(g_{V_i^0}^{(V^0)} g_{A_i^0}^{(V^0)}) (g_{V_j^0}^{(V^0)} g_{A_j^0}^{(V^0)})}{M_i^2 M_j^2} \\ B_{22}(q^2; M_i, M_j) - (M_i^2 + M_j^2) B_0(q^2; M_i, M_j) ; \quad (86)$$

$$\text{fB}_{3;ij}^{\text{CC}} g = \text{fB}_{2;ij}^{\text{NC}} g \quad (\text{with } i \neq j) ; \quad (87)$$

$$\text{fB}_{4;ij}^{\text{CC}} g = \frac{g_{V_i^0}^2 g_{V_j^0}^2}{(2 - \frac{1}{2})^2} \frac{(g_{V_i^0}^{(V^0)} g_{A_i^0}^{(V^0)})^2}{M_i^2 M_j^2} \\ B_{22}(q^2; M_i, M_j) - (M_i^2 + M_j^2) B_0(q^2; M_i, M_j) ; \quad (88)$$

$$\text{fB}_{5;ij}^{\text{CC}} g = \frac{g_{V_i^0}^2 g_{V_j^0}^2}{(2 - \frac{1}{2})^2} \frac{(g_{V_i^0}^{(V^0)} g_{A_i^0}^{(V^0)})^2}{M_i^2 M_j^2} \\ B_{22}(q^2; M_i, M_j) - (M_i^2 + M_j^2) B_0(q^2; M_i, M_j) ; \quad (89)$$

Finally, in terms of these amplitudes, the total pinch contribution from box corrections is given by:

$$\text{fB}_W g = \sum_i \text{fB}_{1;ij}^{\text{CC}} g + \sum_{i,j} \text{fB}_{2;ij}^{\text{CC}} g + \text{fB}_{3;ij}^{\text{CC}} g + \text{fB}_{4;ij}^{\text{CC}} g + \text{fB}_{5;ij}^{\text{CC}} g ; \quad (90)$$

## VI. THE GAUGE BOSON SELF-ENERGIES IN THE PT

In this section, we demonstrate how to construct the self-energies for the SM-like gauge bosons using the various pieces calculated in the previous sections. We will do this first for a general model and then, in the next section, apply our results to the three site model. As stated earlier, we consider the process  $\gamma^*(p_1) + \gamma^*(p_3) \rightarrow \gamma^*(p_2) + \gamma^*(p_4)$  for the neutral currents and the process  $\gamma^*(p_1) + \gamma^*(p_3) \rightarrow \gamma^*(p_2) + Z(p_4)$  for the charged current where both the neutral and charged gauge bosons are exchanged in the t-channel as depicted in Figs. 4 and 8 respectively. The results given below, however, are independent of the particular process [30].



## A . The Neutral Gauge Boson Self-energies

Let us begin by constructing the the PT self-energy for the photon. The tree-level amplitude for the t-channel exchange of a photon is given by:

$$A^0 = \frac{ie^2}{q^2} ; \quad (91)$$

where we have made use of Eq. (7). The amplitude from the loop-corrected photon propagator diagrams takes the form :

$$A^S = \frac{ie^2}{q^2} ; \quad \frac{1}{q^2} A^0 \frac{1}{q^2} ; \quad (92)$$

where represents the sum of the diagrams contributing to the photon's two-point function as given by Eq. (39).

Next, we consider the pinch pieces coming from the ``vertex corrections. In this case, we sum the two middle diagrams of Fig. 4 to find:

$$A^V = 2 \frac{ie^2}{q^2} ; \quad fV g = 2A^0 fV g ; \quad (93)$$

where  $fV g$  represents the pinch contributions from the diagrams in Fig. 6 which are calculated by using Eqs. (49)–(59). The factor of two accounts for the contribution from both ``vertices.

Finally, for the box corrections, we have the amplitude:

$$A^B = \frac{ie^2}{q^2} ; \quad q^2 fB g = A^0 q^2 fB g ; \quad (94)$$

where  $fB g$  represents the pinch contributions coming from the diagrams shown in Fig. 7.

Now, we can construct the photon's self-energy using the PT. Summing Eqs. (92), (93) and (94), we find for the PT loop-corrected amplitude [30, 32]:

$$A^{\text{one loop}} = \frac{A^0}{q^2} + 2q^2 fV g + q^4 fB g$$

$$\frac{A^0}{q^2} \quad \text{PT} : \quad (95)$$

The calculation of the PT self-energy for the Z follows along the same lines as that of the photon. Tree-level exchange of a Z boson in the t-channel results in the amplitude:

$$A_Z^0 = \frac{ig_{\gamma Z}^2}{q^2 - M_Z^2} \quad Z \rightarrow Z ; \quad (96)$$

Then, in terms of Eq. (96), the amplitudes for the loop-corrected Z boson propagator, vertex and box diagrams are given respectively by:

$$A_Z^S = \frac{ig_Z^2}{q^2 M_Z^2} \epsilon_{\mu\nu} \epsilon_{\mu\nu}; \quad \frac{ZZ}{q^2 M_Z^2} A_Z^0 \frac{ZZ}{q^2 M_Z^2}; \quad (97)$$

$$A_Z^V = 2 \frac{ig_Z^2}{q^2 M_Z^2} \epsilon_{\mu\nu} \epsilon_{\mu\nu}; \quad fV_Z g \quad 2A_Z^0 fV_Z g; \quad (98)$$

$$A_Z^B = \frac{ig_Z^2}{q^2 M_Z^2} \epsilon_{\mu\nu} \epsilon_{\mu\nu}; \quad (q^2 - M_Z^2) fB_Z g \quad A_Z^0 (q^2 - M_Z^2) fB_Z g; \quad (99)$$

where the quantities  $\epsilon_{\mu\nu}$ ,  $fV_Z g$  and  $fB_Z g$  can be calculated using the results from Section IV and the factor of two in Eq. (98) accounts for both of the Z ``vertices. Summing Eqs. (97)–(99), the PT one-loop corrected amplitude takes the form :

$$A_Z^{\text{one-loop}} = \frac{A_Z^0}{q^2 M_Z^2} \epsilon_{\mu\nu} \epsilon_{\mu\nu}; \quad (100)$$

where the Z PT self-energy is given by [30, 32]:

$$\epsilon_{\mu\nu}^{\text{PT}} = \epsilon_{\mu\nu} + 2 (q^2 - M_Z^2) fV_Z g + (q^2 - M_Z^2)^2 fB_Z g; \quad (101)$$

The calculation of the PT Z mixing self-energy follows in complete analogy to the cases of the photon and Z self-energies with the exception that there are no tree-level exchange diagrams. The one-loop diagrams which mix the photon and Z propagators give rise to the amplitude:

$$A_Z^S = \frac{ieg_{\gamma Z}}{q^2 (q^2 - M_Z^2)} \epsilon_{\mu\nu} \epsilon_{\mu\nu}; \quad \epsilon_{\mu\nu} : \quad (102)$$

The pinch contributions from vertex corrections are found by summing the second and third diagrams in Fig. 4:

$$A_Z^V = \frac{ieg_{\gamma Z}}{q^2 (q^2 - M_Z^2)} \epsilon_{\mu\nu} \epsilon_{\mu\nu}; \quad (q^2 - M_Z^2) fV_Z^{(1)} g + q^2 fV_Z^{(2)} g; \quad (103)$$

where  $fV_Z^{(1)} g$  comes from the  $\epsilon_{\mu\nu}$  pieces of the ``vertex corrections and  $fV_Z^{(2)} g$  comes from the  $\epsilon_{\mu\nu}$  pieces of the Z ``corrections (see Eqs. (45)–(48)). Lastly, the pinch contributions to the Z mixing arising from box corrections is:

$$A_Z^B = \frac{ieg_{\gamma Z}}{q^2 (q^2 - M_Z^2)} \epsilon_{\mu\nu} \epsilon_{\mu\nu}; \quad q^2 (q^2 - M_Z^2) fB_Z g; \quad (104)$$

Thus, summing Eqs. (102), (103) and (104), the Z mixing PT self-energy can be extracted and we find [30, 32]:

$$\epsilon_{\mu\nu}^{\text{PT}} = \epsilon_{\mu\nu} + (q^2 - M_Z^2) fV_Z^{(1)} g + q^2 fV_Z^{(2)} g + q^2 (q^2 - M_Z^2) fB_Z g; \quad (105)$$

### B . The W Boson Self-energy

We now consider the PT self-energy for the W boson. The amplitude for tree-level W-exchange in t-channel  $\gamma\gamma$  scattering is given by:

$$A_W^0 = \frac{ig_W^2}{q^2 - M_W^2} \gamma_\mu \gamma_\nu ; \quad (106)$$

As in the neutral current cases, the one-loop corrections to the W boson propagator, as well as the pinch contributions from the vertex and box corrections, are proportional to the tree-level amplitude  $A_W^0$ :

$$A_W^S = \frac{ig_W^2}{q^2 - M_W^2} \gamma_\mu \gamma_\nu ; \quad \frac{W W}{q^2 - M_W^2} A_W^0 \frac{W W}{q^2 - M_W^2} ; \quad (107)$$

$$A_W^V = 2 \frac{ig_W^2}{q^2 - M_W^2} \gamma_\mu \gamma_\nu ; \quad fV_W g = 2A_W^0 fV_W g ; \quad (108)$$

$$A_W^B = \frac{ig_W^2}{q^2 - M_W^2} \gamma_\mu \gamma_\nu ; \quad fB_W g = A_W^0 fB_W g ; \quad (109)$$

where the factor of two in  $A_W^V$  accounts for both loop-corrected W  $\gamma\gamma$  vertices. Then, summing Eqs. (107)–(109), the PT one-loop corrected amplitude is given by:

$$A_W^{\text{one-loop}} = \frac{A_W^0}{q^2 - M_W^2} \gamma_\mu \gamma_\nu ; \quad (110)$$

where the W PT self-energy is defined to be [30, 32, 33]:

$$\gamma_\mu \gamma_\nu \gamma_\rho \gamma_\sigma = \gamma_\mu \gamma_\nu + 2(q^2 - M_W^2) fV_W g + (q^2 - M_W^2)^2 fB_W g ; \quad (111)$$

### C . The S and T Parameters in the PT

Finally, having constructed the PT expressions for the self-energies, we can calculate the one-loop corrections to the oblique parameters [29]. Since most experimental analyses require  $U = 0$  [67], we will focus on the calculation of the S and T parameters.

In the PT framework, gauge-invariant expressions for the oblique parameters are constructed by replacing the self-energies calculated from two-point functions alone by their PT counterparts [31]. In other words, using the standard definitions of the S and T parameters from Ref. [29], the PT versions of the S and T parameters are:

$$\frac{S}{4s_W^2 c_W^2} = \frac{P_{ZZ}^{T0}(0)}{P_{ZZ}^{T0}(0)} - \frac{c_W^2}{s_W c_W} \frac{S_Z^2}{P_{ZZ}^{T0}(0)} ; \quad (112)$$

and:

$$T = \frac{\frac{P^T}{W W}(0)}{M_W^2} - \frac{\frac{P^T}{Z Z}(0)}{M_Z^2}; \quad (113)$$

where primes indicate the derivative with respect to  $q^2$  and the PT self-energies  $\frac{P^T}{W W}(q^2)$ ;  $\frac{P^T}{Z Z}(q^2)$ ;  $\frac{P^T}{Z W}(q^2)$  and  $\frac{P^T}{W W}(q^2)$  are given by Eqs. (95), (101), (105) and (111), respectively.

In the following numerical analysis, we define  $c_w$  and  $s_w$  to take their on-shell values, i.e.:

$$c_w^2 = \frac{M_W^2}{M_Z^2} \quad (114)$$

$$s_w^2 = 1 - \frac{M_W^2}{M_Z^2}; \quad (115)$$

while we take the other parameters to be [67]:

$$M_Z = 91.1876 \text{ GeV} \quad (116)$$

$$M_W = 80.385 \text{ GeV} \quad (117)$$

$$M_Z = 91.1876 \text{ GeV} : \quad (118)$$

## VII. RESULTS FOR THE THREE SITE HIGGSLESS MODEL

In this section, we calculate the one-loop, chiral-logarithmic corrections to the  $S$  and  $T$  parameters in the three site Higgsless model. To first approximation, the three site model contains three fundamental scales as depicted in Fig. 12: the mass of the SM-like  $W$ , the mass of the heavy charged gauge boson  $W^0$  and the cutoff scale of the effective theory  $\Lambda$ . In order to estimate the size of the one-loop contributions in this model, we assume that the hierarchy is such that  $M_W^2 \ll M_{W^0}^2 \ll \Lambda^2$ . In this scenario, contributions to the one-loop corrected  $S$  and  $T$  parameters are then dominated by the leading chiral logarithms and any constant term may safely be neglected [68, 69, 70].

To extract the leading chiral logarithms, we apply the following algorithm. First, all tensor integral coefficients are written in terms of scalar integrals as given by Eqs. (A 9)–(A 11) in Appendix A [66]. Then, using Eqs. (A 3) and (A 4), the poles in  $\epsilon$  are identified with the appropriate chiral logarithms. In particular, chiral logarithms coming from diagrams which contain only light, SM-like particles are scaled from the cutoff down to  $M_W$ , while poles originating from diagrams which contain at least one heavy VGB (either  $W^0$  or  $Z^0$ ) are identified with the logarithm  $\log(\Lambda^2/M_{W^0}^2)$ .

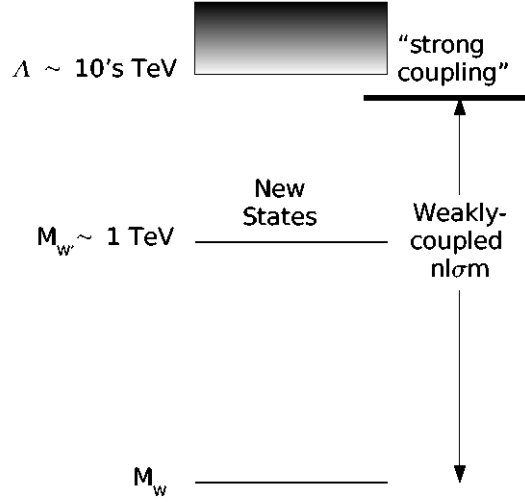


FIG. 12: Fundamental scales of the three site model which are relevant to the calculation of the chiral-logarithmic corrections to the  $S$  and  $T$  parameters.

Finally, in the limit  $M_W^2 \rightarrow M_{W^0}^2$ , the couplings of the  $U(1)$  and the  $SU(2)_2$  gauge groups reduce to the corresponding SM values (up to corrections of  $O(M_W^2 - M_{W^0}^2)$ ) [16, 22]:

$$g^0 = \frac{e}{c_w} ; \quad g' = \frac{e}{s_w} \quad (119)$$

where we have used the tree-level definitions for  $c_w$  and  $s_w$  given by Eqs. (114) and (115). In the following, we use the exact expressions for the couplings given in Appendix B. The chiral-logarithmic corrections to the  $S$  and  $T$  parameters in the limit  $M_W^2 \rightarrow M_{W^0}^2$  have been previously calculated in Refs. [63] and [15] for the three site model with delocalized fermions. The chiral-logarithmic corrections to the delocalization operators, which are important for a phenomenologically viable theory, were also calculated in these references. We have checked that our results in the limit  $M_W^2 \rightarrow M_{W^0}^2$  agree with those of Refs. [63] and [15].

Additionally, in our numerical analysis, we will assume that the mass separation between the  $W^0$  and the  $Z^0$  is identical to the difference between the  $W$  and  $Z$  masses, i.e.  $M_{W^0}^2 - M_Z^2 = M_W^2 - M_Z^2$ . This relation results in maximal suppression of unitarity-violating terms in  $W_L W_L$  scattering [16].

## A . The S Parameter

In the three site Higgsless model with localized fermions, the S parameter receives large corrections at tree-level given by [14, 16, 22]:

$$S_{\text{tree}} = \frac{4s_W^2 M_W^2}{M_{W^0}^2} + \mathcal{O}\left(\frac{M_W^4}{M_{W^0}^4}\right) : \quad (120)$$

When compared to experimental constraints,  $S_{\text{tree}}$  can only be made to agree with the data for  $M_{W^0} \gtrsim 3 \text{ TeV}$  (see Fig. 14). This spoils the restoration of unitarity in  $V_L V_L$  scattering (where  $V = W, Z$ ) which requires  $M_{W^0, Z^0} \gtrsim 1.5 \text{ TeV}$ . Allowing the fermions to have a small (but non-zero) coupling to the additional  $SU(2)$  gauge group provides a negative contribution to  $S_{\text{tree}}$  which, in the ideal case, can vanish altogether [28]. Thus, assessing the one-loop corrections to the S parameter in these models becomes an important issue.

Using the generic results for the PT self-energies from the previous sections and identifying poles in  $\Pi$  with the appropriate chiral logarithms as discussed above, the loop-corrected S parameter in the three site model can be written as:

$$\begin{aligned} S_{3\text{-site}} &= S_{\text{tree}} + A_W^S \log \frac{M_W^2}{M_{W^0}^2} + A_{W^0}^S \log \frac{M_{W^0}^2}{M_{W^0}^2} + S_0 \\ &= S_{\text{tree}} + A_W^S \log \frac{M_W^2}{M_{W^0}^2} + (A_{W^0}^S + A_W^S) \log \frac{M_{W^0}^2}{M_{W^0}^2} + S_0 \end{aligned} \quad (121)$$

where the second term represents the contributions from the low-energy region (below  $M_{W^0}$ ), the third term comprises the high-energy contributions and  $S_0$  represents contributions from higher-dimension operators. Specifically,  $S_0$  arises from the first two operators of Eq. (16). Inserting the expressions for the gauge fields in terms of the mass eigenstates (Eqs. (20)–(22)) into these operators, we can isolate shifts to the kinetic energy terms of the mass eigenstates. The effective Lagrangian describing these shifts takes the form [71]:

$$\mathcal{L}_{S_0} = \frac{A}{4} F_\mu F^\mu + \frac{C}{4} Z_\mu Z^\mu + \frac{G}{2} F_\mu Z^\mu ; \quad (122)$$

where  $F_\mu$  and  $Z_\mu$  are the usual Abelian field strengths and the coefficients  $A, C$  and  $G$  in the three site model are found to be:

$$A = 2 \left( {}_{(1)1} b_{10} b_{20} + {}_{(2)1} b_{00} b_{10} \right) ; \quad (123)$$

$$C = 2 \left( {}_{(1)1} b_{12} b_{22} + {}_{(2)1} b_{02} b_{12} \right) ; \quad (124)$$

$$G = {}_{(1)1} (b_{10} b_{22} + b_{12} b_{20}) + {}_{(2)1} (b_{00} b_{12} + b_{02} b_{10}) ; \quad (125)$$

Finally, in terms of these coefficients, the contribution to  $S$  from higher-dimension operators is [71]:

$$S_0 = \frac{4s_w^2 c_w^2}{S_w C_w} A - C - \frac{c_w^2}{S_w C_w} \frac{s_w^2}{G} G : \quad (126)$$

At this point, an important check on our calculation is the numerical value of the coefficient ( $A_W^S$ ) of the low-energy contribution. Below  $M_{W^0}$ , the symmetries of the three site model are the same as those of the SM with a heavy Higgs boson [11, 12]. This implies the dimension-two interactions in the two models at low energy are identical which, in turn, requires that the chiral-logarithmic corrections calculated from these interactions take the same form in the two theories [72, 73, 74, 75]. One would therefore expect that, in the limit that  $M_W^2 \rightarrow M_{W^0}^2$ , the coefficient of the low-energy contribution in the three site model should reduce to the value one would obtain in the SM with a heavy Higgs boson, i.e. [29, 76, 77, 78, 79, 80]:

$$A_{SM}^S = \frac{1}{12} : \quad (127)$$

In the top panel of Fig. 13, we plot  $A_W^S$  as a function of  $M_{W^0}$ . Clearly,  $A_W^S$  saturates at the SM value for masses  $M_{W^0} \gtrsim 2$  TeV such that we find it useful to rewrite  $A_W^S$  as:

$$A_W^S = \frac{1}{12} + \delta S ; \quad (128)$$

where  $\delta S$  represents the contributions which decouple in the  $M_{W^0} \rightarrow \infty$  limit.

Precision electroweak data can now be used to constrain  $S_{3 \text{ site}}$  and, consequently, some of the relevant parameters ( $M_{W^0}$ ; or the  $(i)1$  coefficients). Although we will not perform the full analysis here, we will outline the steps one must take. The physically-allowed region for  $S$  (and  $T$ ) can be extracted by performing a  $\chi^2$  fit to fourteen precisely measured electroweak observables [81, 82]. Historically, most global analyses of the data have been performed in the context of the SM with a fundamental Higgs boson. However, these analyses can easily be converted to the Higgsless case by first subtracting the chiral-logarithmic contribution from a heavy Higgs boson [29, 76, 77, 78, 79, 80, 83]:

$$S_{H \text{ iggs}} = \frac{1}{12} \log \frac{M_H^2}{M_W^2} ; \quad (129)$$

and then adding back in the contribution from Eq. (121). Thus, the value of the  $S$  parameter to be used in the  $\chi^2$  fit is:

$$\begin{aligned} S(S_0; M_{W^0}; \delta S) &= S_{\text{ref}}(M_H; M_H^{\text{ref}}) - S_{H \text{ iggs}} + S_{3 \text{ site}} \\ &\quad S_{\text{ref}}(M_H; M_H^{\text{ref}}) + S_0 + S_{1 \text{ loop}} ; \end{aligned} \quad (130)$$

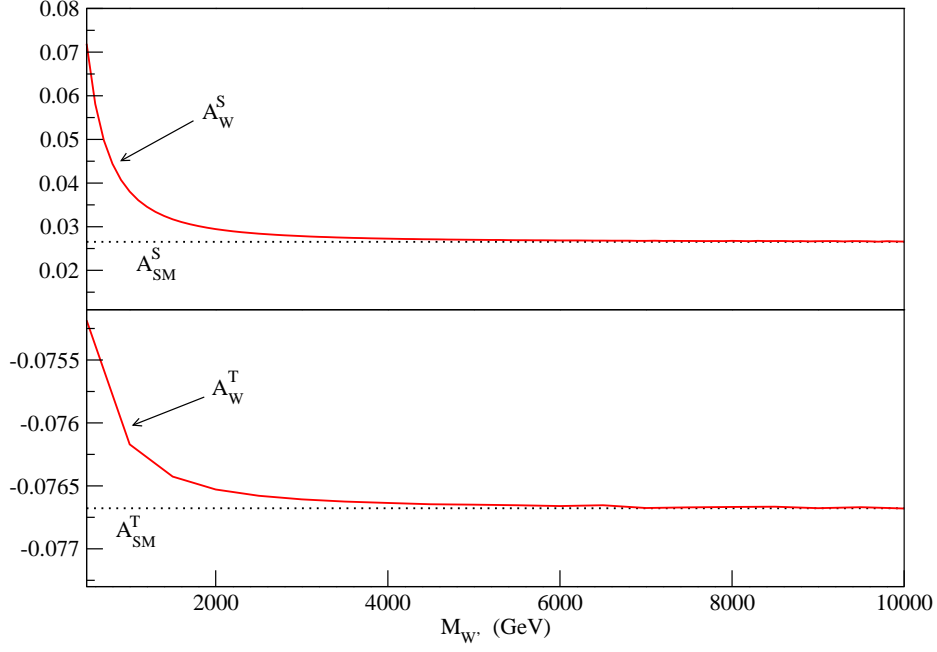


FIG. 13: Top (Bottom) Panel: Coefficient for the low-energy contribution to  $S_{3 \text{ site}}$  ( $T_{3 \text{ site}}$ ) as a function of the  $W^0$  mass.

where  $S_{\text{ref}}(M_H; M_H^{\text{ref}})$  is the SM  $S$  parameter as a function of the physical Higgs boson mass defined with respect to the reference value  $M_H^{\text{ref}}$ . The total one-loop contribution  $S_{1 \text{ loop}}$  from the three site model is:

$$S_{1 \text{ loop}} = S_{\text{tree}} + S \quad (131)$$

and  $S$ , the contribution from the loop diagrams alone, is found to be:

$$S = \frac{1}{12} \log \frac{M_{W^0}^2}{M_{H \text{ ref}}^2} + s \log \frac{M_{W^0}^2}{M_{W^-}^2} + A_{W^0}^S \log \frac{M_{W^0}^2}{M_{W^0}^2} : \quad (132)$$

In Fig. 14, we plot the tree-level and loop-corrected values for the  $S$  parameter in the three site model as functions of  $M_{W^0}$  as well as the cutoff scale  $\Lambda$ . The upper limits of the bands are obtained with  $M_{H \text{ ref}} = 117 \text{ GeV}$ , while the lower limits are obtained with  $M_{H \text{ ref}} = 300 \text{ GeV}$ . In addition, we also show the approximate scale at which unitarity is violated in longitudinal VGB scattering (vertical dotted line) and the 95% C.L. upper limits on the  $S$  parameter for  $M_{H \text{ ref}} = 117 \text{ GeV}$  (upper dashed line) and  $M_{H \text{ ref}} = 300 \text{ GeV}$  (lower dashed



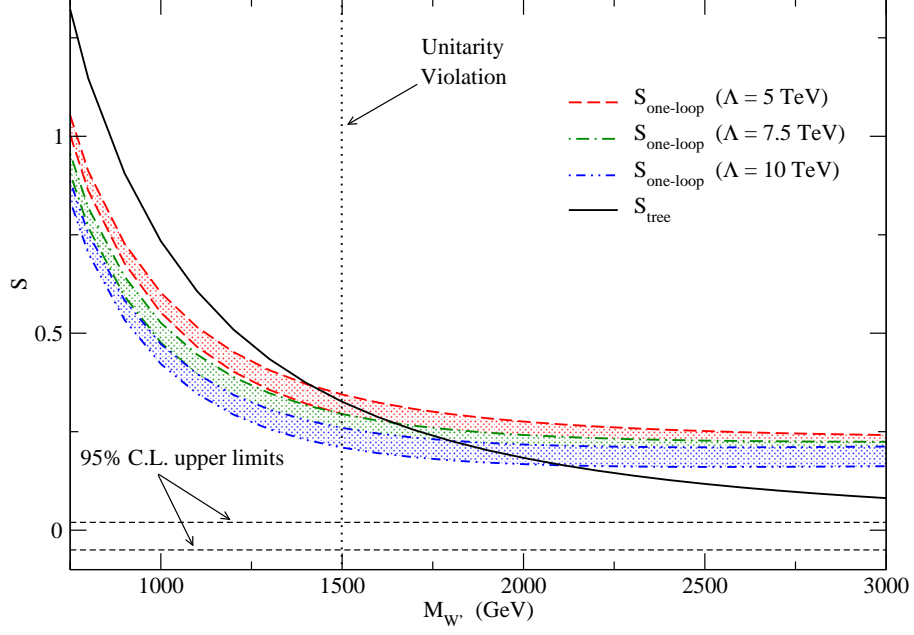


FIG. 14: The  $S$  parameter in the three site Higgsless model at the tree- and one-loop level for different values of the cutoff of the effective theory,  $\Lambda$ . The upper (lower) limit of the bands correspond to the value  $M_{H, \text{ref}} = 117$  (300) GeV. The vertical dotted line represents the approximate scale at which unitarity is violated in longitudinal VGB scattering. The upper (lower) horizontal dashed line represents the 95% C.L. upper limit on  $S$  for  $M_{H, \text{ref}} = 117$  (300) GeV [67].

line) [67]. Although our calculation is not directly comparable to these limits since the coefficients of the higher-dimension operators are unknown, they do serve as an approximate indicator of how well the three site model compares with precision electroweak data. Below the scale of unitarity violation, the one-loop corrections reduce the overall contribution to the  $S$  parameter. However, this reduction is probably not sufficient to overcome the large positive contribution from the tree level.

## B. The T Parameter

At tree level, the T parameter exactly vanishes in the three site model due to the presence of an  $SU(2)$  custodial symmetry. The one-loop, chiral-logarithmic corrections to T naturally separate into low- and high-energy contributions:

$$\begin{aligned} T_{3\text{-site}} &= A_W^T \log \frac{M_W^2}{M_{W^0}^2} + A_{W^0}^T \log \frac{M_W^2}{M_{W^0}^2} + T_0 \\ &= A_W^T \log \frac{M_{W^0}^2}{M_W^2} + (A_{W^0}^T + A_W^T) \log \frac{M_W^2}{M_{W^0}^2} + T_0; \end{aligned} \quad (133)$$

where  $T_0$  represents the contribution from the dimension-two operator of Eq. (14). The expression for  $T_0$  can be extracted by inserting the expansions of the gauge fields in terms of the mass eigenstates (Eqs. (20) and (21)) into Eq. (14). Isolating corrections to the SM-like Z boson mass, we find that  $L_2^0$  produces a term of the form:

$$L_{T^0} = -\frac{z}{2} M_Z^2 Z^\mu Z_\mu; \quad (134)$$

where  $z$  is given by:

$$z = \frac{(2) f_1^2}{2M_Z^2} (g^0 b_{02} - g b_{12})^2; \quad (135)$$

In contrast, higher-dimension operators do not contribute to a shift in the W boson mass and  $T_0$  is given by [71]:

$$T_0 = -z = -\frac{(2) f_1^2}{2M_Z^2} (g^0 b_{02} - g b_{12})^2; \quad (136)$$

As a check of our calculation for T in the three site model, we plot the coefficient of the low-energy contribution,  $A_W^T$ , in the bottom panel of Fig. (13). In the energy region below  $M_{W^0}$ , the operators which generate corrections to T in the three site model are identical to the operators of the SM with a heavy Higgs boson [72, 73, 74, 75]. Therefore, in the limit  $M_W^2 \rightarrow M_{W^0}^2$ ,  $A_W^T$  reduces to the SM value: [29, 76, 77, 78, 79, 80]:

$$A_{SM}^T = \frac{3}{16 c_w^2}; \quad (137)$$

as seen in the bottom panel of Fig. (13). Thus, to simplify our analysis, we find it convenient to rewrite the low-energy coefficient as:

$$A_W^T = \frac{3}{16 c_w^2} + T; \quad (138)$$

where  $T$  parameterizes the piece of the low-energy contributions which decouple in the large  $M_{W^0}$  limit.

In analogy to the previous section, the one-loop prediction for  $T$  can now be compared to precision electroweak data in order to constrain some (or all) of the parameters of the three site model. The analysis follows along the same lines as the case of the  $S$  parameter. First, the chiral-logarithmic contribution from a heavy Higgs boson [29, 76, 77, 78, 79, 80, 83]:

$$T_{\text{Higgs}} = \frac{3}{16 c_W^2} \log \frac{M_H^2}{M_{W^0}^2} ; \quad (139)$$

must be subtracted from the global analysis. Then, adding back in the contribution from Eq. (133), the value of  $T$  to be used in the  $\chi^2$  fit is given by:

$$T(T_0; M_{W^0}; \mu) = T_{\text{ref}}(M_H; M_H^{\text{ref}}) - T_{\text{Higgs}} + T_{3\text{-site}} \quad (140)$$

$$T_{\text{ref}}(M_H; M_H^{\text{ref}}) + T_0 + T_{\text{one-loop}} ; \quad (141)$$

where  $T_{\text{ref}}(M_H; M_H^{\text{ref}})$  is the SM  $T$  parameter as a function of the physical Higgs boson mass defined with respect to the reference value  $M_H^{\text{ref}}$  and  $T_{\text{one-loop}}$  is found to be:

$$T_{\text{one-loop}} = \frac{3}{16 c_W^2} \log \frac{M_{W^0}^2}{M_H^2} + T \log \frac{M_{W^0}^2}{M_H^2} + A_{W^0}^T \log \frac{M_{W^0}^2}{M_{W^0}^2} : \quad (142)$$

In Fig. 15, we plot  $T_{\text{one-loop}}$  as a function of  $M_{W^0}$  and  $\mu$ . The lower (upper) curves are obtained with a reference Higgs boson mass of 117 (300) GeV. The dashed vertical line indicates the approximate scale of unitarity violation in longitudinal VGB scattering, while the 95% C.L. lower limit on  $T$  with  $M_{H,\text{ref}} = 117$  (300) GeV is shown as the lower (upper) horizontal dashed line. As before, these limits provide an approximate benchmark to which our calculation can be compared.

First, in contrast to the case of the  $S$  parameter, we see that the one-loop corrections to  $T$  are consistent with the constraints from unitarity violation in that lighter masses are preferred. More interesting, though, is the near independence of the one-loop corrections on the cutoff scale which indicates that the sum of the coefficients in Eq. (142) nearly vanishes, i.e.:

$$A_{W^0}^T + A_W^T \approx 0 ; \quad (143)$$

over the full mass range considered. This result, along with the fact that  $T$  vanishes in the large  $M_{W^0}$  limit, implies that one-loop corrections are dominated by the first term in

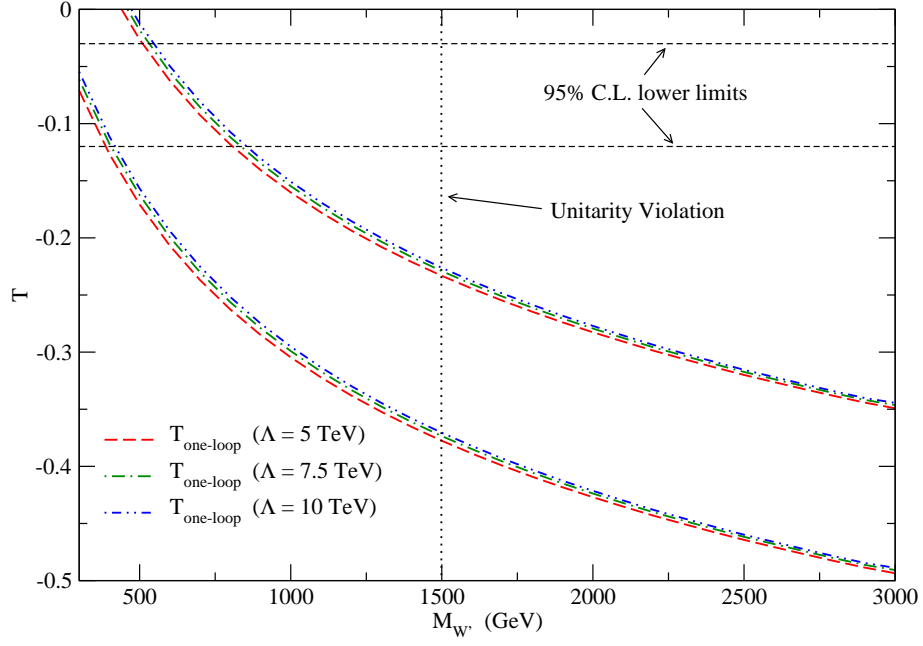


FIG. 15: One-loop, chiral-logarithmic corrections to the  $T$  parameter in the three site model as a function of  $M_{W^0}$  and  $\Lambda$ . The lower (upper) curves correspond to  $M_{H,ref} = 117$  (300) GeV. The vertical dotted line represents the approximate scale of unitarity violation in  $V_L V_L$  ( $V = W, Z$ ) scattering. The lower (upper) horizontal dashed lines represent the 95% C.L. lower limits of the  $T$  parameter for  $M_{H,ref} = 117$  (300) GeV.

Eq. (142) which arises due to the "mismatch" between the Higgs boson and  $W^0$  masses. Thus, in the situation where these masses are equal, the one-loop contributions to the  $T$  parameter vanish due to the custodial  $SU(2)$  symmetry in the three site model.

### VIII. CONCLUSIONS

In this paper, we calculated the one-loop contributions from vector gauge bosons to the  $S$  and  $T$  parameters in Higgsless models with extra dimensions or extended gauge symmetries using a novel application of the Pinch Technique. We performed this calculation in terms of generic Feynman rules and couplings, such that our results can be applied to a variety of

models. As an example, we applied our calculation to the case of the highly-deconstructed three site Higgsless model with localized fermions. The low-energy sector of this model has the same gauge and chiral symmetries as the SM with a heavy Higgs boson which implies that the contributions from this sector to electroweak parameters are the same.

The chiral-logarithmic corrections to the  $S$  parameter in the three site model were found to be negative in the energy region below the scale of unitarity violation. The reduction is not enough to overcome the large positive tree-level contribution and so this model exhibits the tension between unitarity constraints and constraints from the  $S$  parameter which is present in most Higgsless models. However, by delocalizing the fermions, the  $S$  parameter at tree level can always be made to vanish in this model.

The chiral-logarithmic corrections to the  $T$  parameter, on the other hand, are consistent with constraints from unitarity violation in that lighter masses are required to keep  $T$  within experimental limits. The one-loop corrections are also nearly independent of the cutoff scale over the full mass range considered.

Finally, it should be stated that our calculation is not exclusive to Higgsless models. As mentioned in the Introduction, one-loop corrections to the VGB self-energies can always be separated into gauge-invariant contributions from fermions, scalars and gauge bosons. In other words, our calculation could be used to calculate the gauge-bosonic contributions to oblique parameters in models which contain fundamental (or composite) Higgs bosons.

#### Acknowledgments

We are very grateful to Sekhar Chivukula and Shinya Matsuzaki for useful discussions on the three site model. We would also like to thank Hooman Davoudiasl for a careful reading of the manuscript. This manuscript has been authored by employees of Brookhaven Science Associates, LLC under Contract No. DE-AC02-98CH10886 with the U.S. Department of Energy. The publisher by accepting the manuscript for publication acknowledges that the United States Government retains a non-exclusive, paid-up, irrevocable, world-wide license to publish or reproduce the published form of this manuscript, or allow others to do so, for United States Government purposes.

The scalar integrals that appear in the calculation of the PT self-energies are the one-point integral  $A_0(M)$ :

$$A_0(M) = \int \frac{d^n k}{(2\pi)^n} \frac{1}{k^2 - M^2}; \quad (\text{A } 1)$$

and the two-point integral  $B_0(q^2; M_1; M_2)$ :

$$B_0(q^2; M_1; M_2) = \int \frac{d^n k}{(2\pi)^n} \frac{1}{(k^2 - M_1^2)((k+q)^2 - M_2^2)}; \quad (\text{A } 2)$$

In order to extract the chiral-logarithmic corrections, we only need to calculate the poles of the scalar integrals which are then identified with the appropriate chiral logarithms:

$$A_0(M)_{\text{pole}} = \frac{i}{16\pi^2} M^2 + \frac{i}{16\pi^2} \log \frac{M^2}{\mu^2}; \quad (\text{A } 3)$$

and:

$$B_0(q^2; M_1; M_2)_{\text{pole}} = \frac{i}{16\pi^2} + \frac{i}{16\pi^2} \log \frac{M^2}{\mu^2}; \quad (\text{A } 4)$$

The tensor integrals that arise in our calculation consist of the rank-one and rank-two two-point integrals:

$$B_1(q^2; M_1; M_2) = \int \frac{d^n k}{(2\pi)^n} \frac{k}{(k^2 - M_1^2)((k+q)^2 - M_2^2)}; \quad (\text{A } 5)$$

$$B_2(q^2; M_1; M_2) = \int \frac{d^n k}{(2\pi)^n} \frac{k k}{(k^2 - M_1^2)((k+q)^2 - M_2^2)}; \quad (\text{A } 6)$$

Tensor integrals can always be expanded in terms of external momenta and the metric tensor  $g$  [66]. Specifically, the integrals in Eqs. (A 5) and (A 6) can be written as

$$B_1(q^2; M_1; M_2) = q_\mu B_{11}(q^2; M_1; M_2) \quad (\text{A } 7)$$

$$B_2(q^2; M_1; M_2) = q_\mu q_\nu B_{21}(q^2; M_1; M_2) + g_{\mu\nu} B_{22}(q^2; M_1; M_2); \quad (\text{A } 8)$$

Finally, equating the tensor integral with its respective expansion and contracting both sides with external momenta and  $g$ , one can solve the system of equations for the coefficients

cients in Eqs. (A 7) and (A 8) in terms of the scalar integrals. Specifically,:

$$B_{11}(q^2; M_1; M_2) = \frac{1}{2q^2} A_0(M_1) - A_0(M_2) - (q^2 + M_1^2 - M_2^2) B_0(q^2; M_1; M_2) \quad (A 9)$$

$$B_{21}(q^2; M_1; M_2) = \frac{1}{3q^2} A_0(M_2) + 2(M_2^2 - M_1^2 - q^2) B_{11}(q^2; M_1; M_2) \\ M_1^2 B_0(q^2; M_1; M_2) \quad (A 10)$$

$$B_{22}(q^2; M_1; M_2) = \frac{1}{3} \frac{1}{2} A_0(M_2) + M_1^2 B_0(q^2; M_1; M_2) \\ \frac{1}{2} (M_2^2 - M_1^2 - q^2) B_{11}(q^2; M_1; M_2) : \quad (A 11)$$

## APPENDIX B: FORMULAE FOR THE THREE SITE MODEL

In this appendix, we summarize the relevant formulae for the three site model [14, 16, 22]. We begin by finding the mass eigenvalues. First, in the charged sector, the mass matrix is:

$$M_{CC} = \frac{1}{4} \begin{pmatrix} 0 & 1 \\ g^2(f_1^2 + f_2^2) & g^2 f_2^2 \\ g^2 f_1^2 & g^2 f_2^2 \end{pmatrix} A; \quad (B 1)$$

for which we find the eigenvalues:

$$M_{W^\pm}^2 = \frac{1}{8} \left[ g^2(f_1^2 + f_2^2) + g^2 f_2^2 \pm \sqrt{(g^2(f_1^2 + f_2^2) + g^2 f_2^2)^2 - 4f_1^2 f_2^2 g^2} \right]^{\frac{1}{2}}; \quad (B 2)$$

where the SM-like  $W$  is identified with the lighter of the two eigenvalues.

Next, the mass matrix for the neutral sector is:

$$M_{NC} = \frac{1}{8} \begin{pmatrix} 0 & 1 \\ g^2 f_1^2 & g^2 f_1^2 & 0 \\ g^2 f_1^2 & g^2(f_1^2 + f_2^2) & g^2 f_2^2 \\ 0 & g^2 f_2^2 & g^2 f_2^2 \end{pmatrix} \begin{pmatrix} B \\ C \\ A \end{pmatrix}; \quad (B 3)$$

Diagonalizing this matrix results in a massless eigenstate, which is identified with the SM photon, and two massive states with mass eigenvalues:

$$M_{Z, Z^0}^2 = \frac{1}{16} \left[ g^2(f_1^2 + f_2^2) + g^2 f_1^2 + g^2 f_2^2 \pm \sqrt{(g^2(f_1^2 + f_2^2) + g^2 f_1^2 + g^2 f_2^2)^2 - 4f_1^2 f_2^2 (g^2 f_1^2 + g^2 f_2^2)} \right]^{\frac{1}{2}}; \quad (B 4)$$

where the SM -like  $Z$  is identified with the lighter of the two states.

In its original form, the three site model contains five free parameters:  $g; g^0; g; f_1$  and  $f_2$ . For our analysis, we find it convenient to exchange these parameters for the four masses ( $M_W; M_Z; M_{W^0}$  and  $M_{Z^0}$ ) defined through Eqs. (B2) and (B4). As the fifth parameter, we choose the electromagnetic coupling  $e$  which is defined by Eq. (17). Solving these equations for the original parameters, we find [16]:

$$\begin{aligned}
g^0 &= \frac{e^2 M_Z^2 M_{Z^0}^2}{M_W^2 M_{W^0}^2}; \\
g^2 &= g^0 \frac{(M_W^2 + M_{W^0}^2)(M_Z^2 + M_{Z^0}^2 - M_W^2 - M_{W^0}^2) + M_W^2 M_{W^0}^2 - M_Z^2 M_{Z^0}^2}{(M_Z^2 + M_{Z^0}^2 - M_W^2 - M_{W^0}^2)^2}; \\
g^2 &= g^0 M_W^2 M_{W^0}^2 \frac{(M_W^2 + M_{W^0}^2)(M_Z^2 + M_{Z^0}^2 - M_W^2 - M_{W^0}^2) + M_W^2 M_{W^0}^2 - M_Z^2 M_{Z^0}^2}{(M_Z^2 - M_W^2)(M_{Z^0}^2 - M_{W^0}^2)(M_{Z^0}^2 - M_W^2)(M_{W^0}^2 - M_Z^2)}; \\
f_1^2 &= \frac{4}{g^0} (M_Z^2 + M_{Z^0}^2 - M_W^2 - M_{W^0}^2); \\
f_2^2 &= \frac{16 M_W^2 M_{W^0}^2}{g^2 g^0 f_1^2}; \tag{B5}
\end{aligned}$$

where we have assumed in the above relations that  $M_{Z^0} > M_{W^0}$ .

Finally, in order to compute the couplings relevant to the calculation of the  $S$  and  $T$  parameters, we need to calculate the mixing angles defined through Eqs. (18)–(22). First, in the charged sector, we have  $a_{11} = a_{22}$  and  $a_{12} = -a_{21}$  where:

$$\begin{aligned}
a_{11} &= \frac{M_{W^0}^2 (M_{W^0}^2 - M_Z^2)(M_{Z^0}^2 - M_{W^0}^2)}{M_{W^0}^2 (M_{W^0}^2 - M_Z^2)(M_{Z^0}^2 - M_{W^0}^2) + M_W^2 (M_{Z^0}^2 - M_W^2)(M_Z^2 - M_W^2)}^{1=2}; \\
a_{12} &= \frac{M_W^2 (M_{Z^0}^2 - M_W^2)(M_Z^2 - M_W^2)}{M_{W^0}^2 (M_{W^0}^2 - M_Z^2)(M_{Z^0}^2 - M_{W^0}^2) + M_W^2 (M_{Z^0}^2 - M_W^2)(M_Z^2 - M_W^2)}^{1=2} : \tag{B6}
\end{aligned}$$



The mixing angles in the neutral sector are given by:

$$b_{00} = \frac{e}{g^0}; \quad (B7)$$

$$b_{10} = \frac{e}{g};$$

$$b_{20} = \frac{e}{g};$$

$$b_{01} = \frac{(M_{Z^0}^2 - M_W^2)(M_{Z^0}^2 - M_{W^0}^2)}{M_{Z^0}^2(M_{Z^0}^2 - M_Z^2)}^{1=2};$$

$$b_{11} = 4 \frac{(M_{Z^0}^2 - M_W^2)(M_{Z^0}^2 - M_{W^0}^2)}{M_{Z^0}^2(M_{Z^0}^2 - M_Z^2)(M_W^2 + M_{W^0}^2)(M_Z^2 + M_{Z^0}^2 - M_W^2 - M_{W^0}^2) + M_W^2 M_{W^0}^2 - M_Z^2 M_{Z^0}^2}^{3_{1=2}};$$

$$b_{21} = 4 \frac{(M_{Z^0}^2 - M_W^2)(M_{Z^0}^2 - M_{W^0}^2)}{M_{Z^0}^2(M_{Z^0}^2 - M_Z^2)(M_W^2 + M_{W^0}^2)(M_Z^2 + M_{Z^0}^2 - M_W^2 - M_{W^0}^2) + M_W^2 M_{W^0}^2 - M_Z^2 M_{Z^0}^2}^{3_{1=2}};$$

$$b_{02} = \frac{(M_Z^2 - M_W^2)(M_{Z^0}^2 - M_Z^2)}{M_Z^2(M_{Z^0}^2 - M_Z^2)}^{1=2};$$

$$b_{12} = 4 \frac{(M_Z^2 - M_W^2)(M_{Z^0}^2 - M_Z^2)}{M_Z^2(M_{Z^0}^2 - M_Z^2)(M_W^2 + M_{W^0}^2)(M_Z^2 + M_{Z^0}^2 - M_W^2 - M_{W^0}^2) + M_W^2 M_{W^0}^2 - M_Z^2 M_{Z^0}^2}^{3_{1=2}};$$

$$b_{22} = 4 \frac{(M_Z^2 - M_W^2)(M_{Z^0}^2 - M_Z^2)}{M_Z^2(M_{Z^0}^2 - M_Z^2)(M_W^2 + M_{W^0}^2)(M_Z^2 + M_{Z^0}^2 - M_W^2 - M_{W^0}^2) + M_W^2 M_{W^0}^2 - M_Z^2 M_{Z^0}^2}^{3_{1=2}};$$

[1] N. Arkani-Hamed, S. Dimopoulos, and G. R. Dvali, Phys. Lett. B 429, 263 (1998), hep-ph/9803315.

[2] L. Randall and R. Sundrum, Phys. Rev. Lett. 83, 3370 (1999), hep-ph/9905221.

[3] C. Csaki, C. Grojean, H. Murayama, L. Pilo, and J. Terning, Phys. Rev. D 69, 055006 (2004), hep-ph/0305237.

- [4] G . Cacciapaglia, C . C saki, C . G rojean, and J . Teming, Phys. Rev. D 71, 035015 (2005), hep-ph/0409126.
- [5] Y . Nomura, JHEP 11, 050 (2003), hep-ph/0309189.
- [6] C . C saki, C . G rojean, L . P ilo, and J . Teming, Phys. Rev. Lett. 92, 101802 (2004), hep-ph/0308038.
- [7] B . W . Lee, C . Quigg, and H . B . Thacker, Phys. Rev. D 16, 1519 (1977).
- [8] N . ArkaniHamed, A . G . Cohen, and H . Georgi, Phys. Rev. Lett. 86, 4757 (2001), hep-th/0104005.
- [9] C . T . Hill, S . Pokorski, and J . Wang, Phys. Rev. D 64, 105005 (2001), hep-th/0104035.
- [10] T . Appelquist and C . W . Bernard, Phys. Rev. D 22, 200 (1980).
- [11] A . C . Longhitano, Phys. Rev. D 22, 1166 (1980).
- [12] A . C . Longhitano, Nucl. Phys. B 188, 118 (1981).
- [13] J . Bagger, S . Dawson, and G . Valencia, Nucl. Phys. B 399, 364 (1993), hep-ph/9204211.
- [14] M . Perelstein, JHEP 10, 010 (2004), hep-ph/0408072.
- [15] R . S . Chivukula, S . Matsuzaki, E . H . Simmons, and M . Tanabashi (2007), hep-ph/0702218.
- [16] R . Foadi, S . Gopalakrishna, and C . Schmidt, JHEP 03, 042 (2004), hep-ph/0312324.
- [17] J . Him and J . Stern, Eur. Phys. J. C 34, 447 (2004), hep-ph/0401032.
- [18] R . Casalbuoni, S . De Curtis, and D . Domini, Phys. Rev. D 70, 055010 (2004), hep-ph/0405188.
- [19] R . S . Chivukula, E . H . Simmons, H .-J . He, M . Kurachi, and M . Tanabashi, Phys. Rev. D 70, 075008 (2004), hep-ph/0406077.
- [20] H . Georgi, Phys. Rev. D 71, 015016 (2005), hep-ph/0408067.
- [21] R . Sekhar Chivukula, E . H . Simmons, H .-J . He, M . Kurachi, and M . Tanabashi, Phys. Rev. D 71, 035007 (2005), hep-ph/0410154.
- [22] R . Sekhar Chivukula et al. (2006), hep-ph/0607124.
- [23] G . Cacciapaglia, C . C saki, C . G rojean, M . Reece, and J . Teming, Phys. Rev. D 72, 095018 (2005), hep-ph/0505001.
- [24] R . Foadi, S . Gopalakrishna, and C . Schmidt, Phys. Lett. B 606, 157 (2005), hep-ph/0409266.
- [25] R . Foadi and C . Schmidt, Phys. Rev. D 73, 075011 (2006), hep-ph/0509071.
- [26] R . S . Chivukula, E . H . Simmons, H .-J . He, M . Kurachi, and M . Tanabashi, Phys. Rev. D 71, 115001 (2005), hep-ph/0502162.

- [27] R. Casalbuoni, S. De Curtis, D. Dolce, and D. Dominici, Phys. Rev. D 71, 075015 (2005), hep-ph/0502209.
- [28] R. Sekhar Chivukula, E. H. Simmons, H.-J. He, M. Kurachi, and M. Tanabashi, Phys. Rev. D 72, 015008 (2005), hep-ph/0504114.
- [29] M. E. Peskin and T. Takeuchi, Phys. Rev. D 46, 381 (1992).
- [30] G. Degrossi and A. Sirlin, Phys. Rev. D 46, 3104 (1992).
- [31] G. Degrossi, B. A. Kniehl, and A. Sirlin, Phys. Rev. D 48, 3963 (1993).
- [32] G. Degrossi and A. Sirlin, Nucl. Phys. B 383, 73 (1992).
- [33] J. Papavassiliou and A. Sirlin, Phys. Rev. D 50, 5951 (1994), hep-ph/9403378.
- [34] J. M. Comwall (1981), UCLA/81/TEP/12.
- [35] J. M. Comwall, Phys. Rev. D 26, 1453 (1982).
- [36] J. M. Comwall and J. Papavassiliou, Phys. Rev. D 40, 3474 (1989).
- [37] J. Papavassiliou, Phys. Rev. D 41, 3179 (1990).
- [38] K. Agashe, A. Delgado, M. J. May, and R. Sundrum, JHEP 08, 050 (2003), hep-ph/0308036.
- [39] R. Barbieri, A. Pomarol, and R. Rattazzi, Phys. Lett. B 591, 141 (2004), hep-ph/0310285.
- [40] C. C. Saki, C. G. rojean, J. Hubisz, Y. Shim an, and J. Teming, Phys. Rev. D 70, 015012 (2004), hep-ph/0310355.
- [41] H. Davoudiasl, J. L. Hewett, B. Lillie, and T. G. Rizzo, Phys. Rev. D 70, 015006 (2004), hep-ph/0312193.
- [42] G. Burdman and Y. Nomura, Phys. Rev. D 69, 115013 (2004), hep-ph/0312247.
- [43] G. Cacciapaglia, C. C. Saki, C. G. rojean, and J. Teming, Phys. Rev. D 70, 075014 (2004), hep-ph/0401160.
- [44] H. Davoudiasl, J. L. Hewett, B. Lillie, and T. G. Rizzo, JHEP 05, 015 (2004), hep-ph/0403300.
- [45] R. Barbieri, A. Pomarol, R. Rattazzi, and A. Strumia, Nucl. Phys. B 703, 127 (2004), hep-ph/0405040.
- [46] K. Agashe, G. Perez, and A. Soni, Phys. Rev. Lett. 93, 201804 (2004), hep-ph/0406101.
- [47] J. L. Hewett, B. Lillie, and T. G. Rizzo, JHEP 10, 014 (2004), hep-ph/0407059.
- [48] K. Agashe, G. Perez, and A. Soni, Phys. Rev. D 71, 016002 (2005), hep-ph/0408134.
- [49] B. Lillie, JHEP 02, 019 (2006), hep-ph/0505074.
- [50] K. Agashe, G. Perez, and A. Soni, Phys. Rev. D 75, 015002 (2007), hep-ph/0606293.
- [51] M. Carena, E. Ponton, J. Santiago, and C. E. M. Wagner, Nucl. Phys. B 759, 202 (2006),

- hep-ph/0607106.
- [52] G . Cacciapaglia, C . C saki, G . M arandella, and J . Teming, Phys. Rev. D 75, 015003 (2007), hep-ph/0607146.
  - [53] A . D juadi, G . M oreau, and F . R ichard (2006), hep-ph/0610173.
  - [54] G . Cacciapaglia, C . C saki, G . M arandella, and J . Teming, JHEP 02, 036 (2007), hep-ph/0611358.
  - [55] R . C ontino, T . K ram er, M . Son, and R . Sundrum (2006), hep-ph/0612180.
  - [56] M . C arena, E . P onton, J . S antiago, and C . E . M . W agner (2007), hep-ph/0701055.
  - [57] B . L illie, L . R andall, and L . T . W ang (2007), hep-ph/0701166.
  - [58] K . A gashe, H . D avoudiasl, G . P erez, and A . S oni (2007), hep-ph/0701186.
  - [59] R . S . C hivukula, H . J . H e, J . H oward, and E . H . S im m ons, Phys. Rev. D 69, 015009 (2004), hep-ph/0307209.
  - [60] R . S . C hivukula, E . H . S im m ons, H . J . H e, M . K urachi, and M . T anabashi, Phys. Lett. B 603, 210 (2004), hep-ph/0408262.
  - [61] R . S . C hivukula, E . H . S im m ons, H . J . H e, M . K urachi, and M . T anabashi, Phys. Rev. D 72, 075012 (2005), hep-ph/0508147.
  - [62] R . S ekhar C hivukula, E . H . S im m ons, H . J . H e, M . K urachi, and M . T anabashi, Phys. Rev. D 72, 095013 (2005), hep-ph/0509110.
  - [63] S . M atsuzaki, R . S . C hivukula, M . T anabashi, and E . H . S im m ons (2006), hep-ph/0607191.
  - [64] R . S ekhar C hivukula, E . H . S im m ons, H . J . H e, M . K urachi, and M . T anabashi, Phys. Rev. D 75, 035005 (2007), hep-ph/0612070.
  - [65] A . B irkedal, K . M atchev, and M . P erelstein, Phys. Rev. Lett. 94, 191803 (2005), hep-ph/0412278.
  - [66] G . P assarino and M . J . G . V eltm an, Nucl. Phys. B 160, 151 (1979).
  - [67] W . M . Y ao et al. (Particle Data G roup), J. Phys. G 33, 1 (2006).
  - [68] L . F . L i and H . P agels, Phys. Rev. Lett. 26, 1204 (1971).
  - [69] L . L ing-Fong and H . P agels, Phys. Rev. D 5, 1509 (1972).
  - [70] P . L angacker and H . P agels, Phys. Rev. D 8, 4595 (1973).
  - [71] C . C saki, J . H ubisz, and P . M eade (2005), hep-ph/0510275.
  - [72] M . B ando, T . K ugo, S . U ehara, K . Y am awaki, and T . Y anagida, Phys. Rev. Lett. 54, 1215 (1985).

- [73] M .Bando, T .Kugo, and K .Yam awaki, Nucl.Phys.B 259, 493 (1985).
- [74] M .Bando, T .Fujwara, and K .Yam awaki, Prog.Theor.Phys. 79, 1140 (1988).
- [75] M .Bando, T .Kugo, and K .Yam awaki, Phys.Rept. 164, 217 (1988).
- [76] M .J.Herrero and E .Ruiz M orales, Nucl.Phys.B 418, 431 (1994), hep-ph/9308276.
- [77] M .J.Herrero and E .Ruiz M orales, Nucl.Phys.B 437, 319 (1995), hep-ph/9411207.
- [78] S.D ittm aier and C .G rosse-K netter, Nucl.Phys.B 459, 497 (1996), hep-ph/9505266.
- [79] J.M atias, Nucl.Phys.B 478, 90 (1996), hep-ph/9604390.
- [80] S.A lam , S.D aw son, and R .Szalapski, Phys.Rev.D 57, 1577 (1998), hep-ph/9706542.
- [81] J.A .Bagger, A .F .Falk, and M .Swartz, Phys.Rev.Lett. 84, 1385 (2000), hep-ph/9908327.
- [82] R .S .Chivukula, C .Hoelbling, and N .J .Evans, Phys.Rev.Lett. 85, 511 (2000), hep-ph/0002022.
- [83] R .S .Chivukula and N .J .Evans, Phys.Lett.B 464, 244 (1999), hep-ph/9907414.